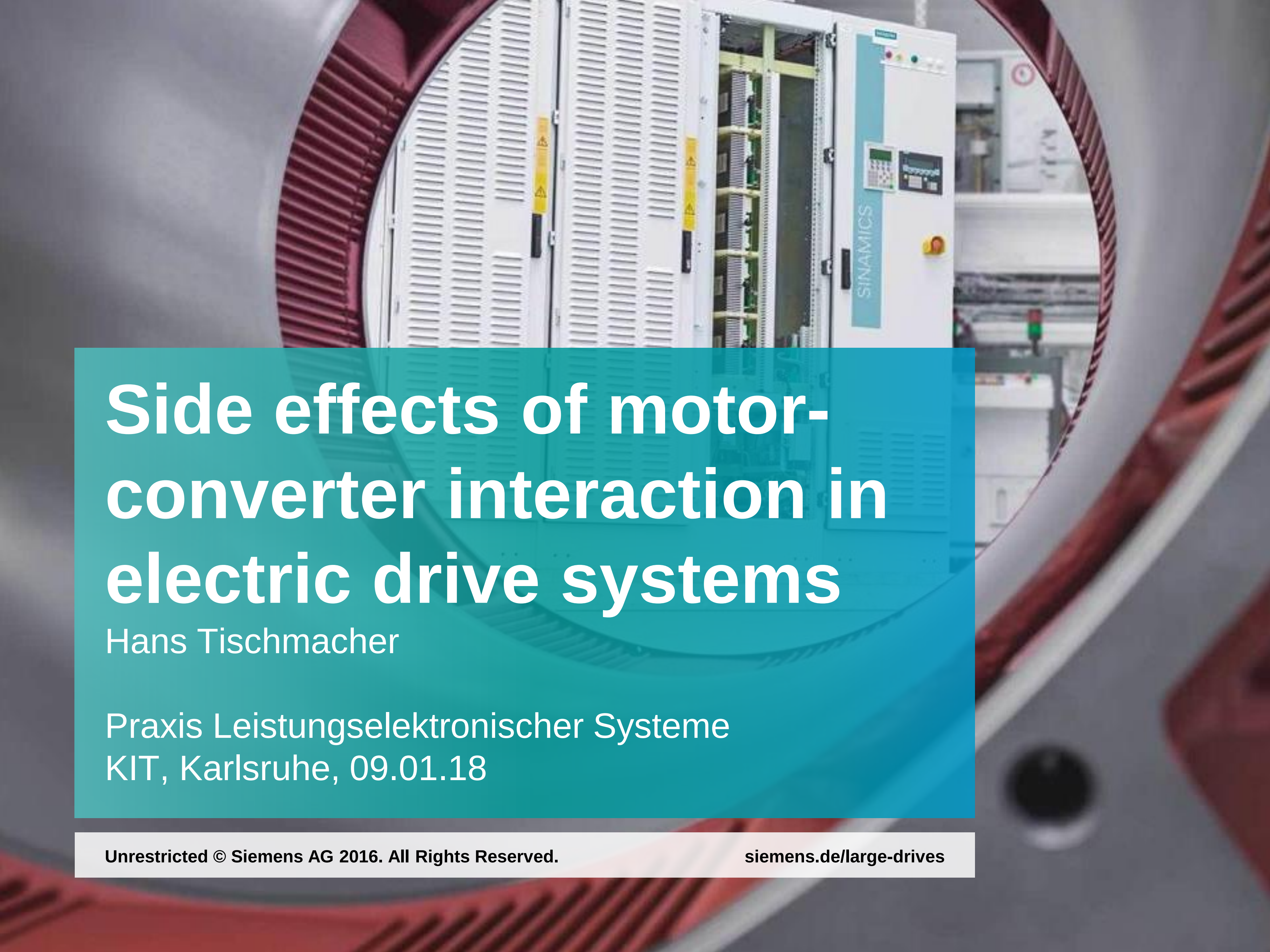

Side effects of motor-converter interaction in electric drive systems

Hans Tischmacher

Praxis Leistungselektronischer Systeme
KIT, Karlsruhe, 09.01.18

Power range and products

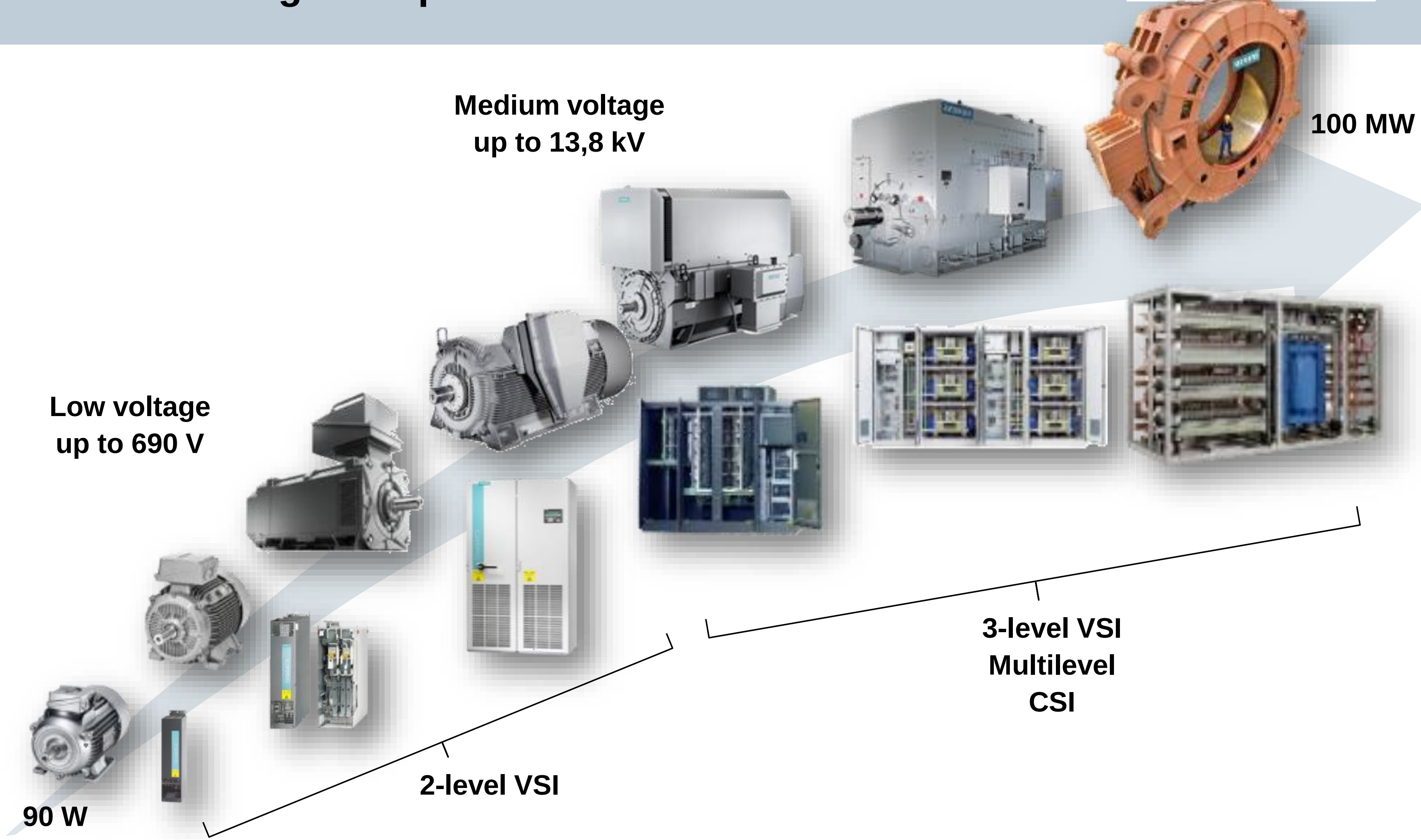

2-level voltage source converter (1)

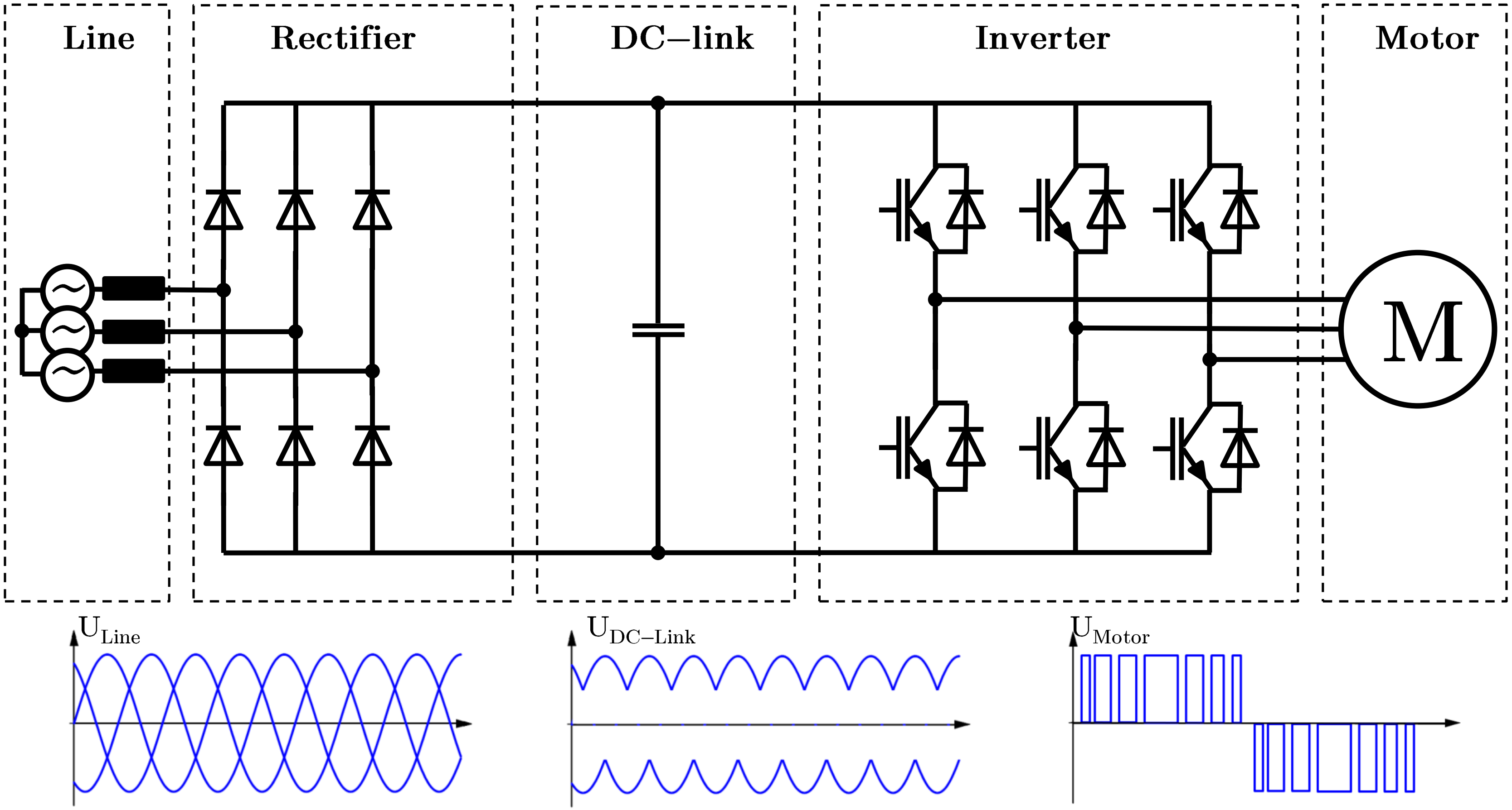

2-level voltage source converter (2)

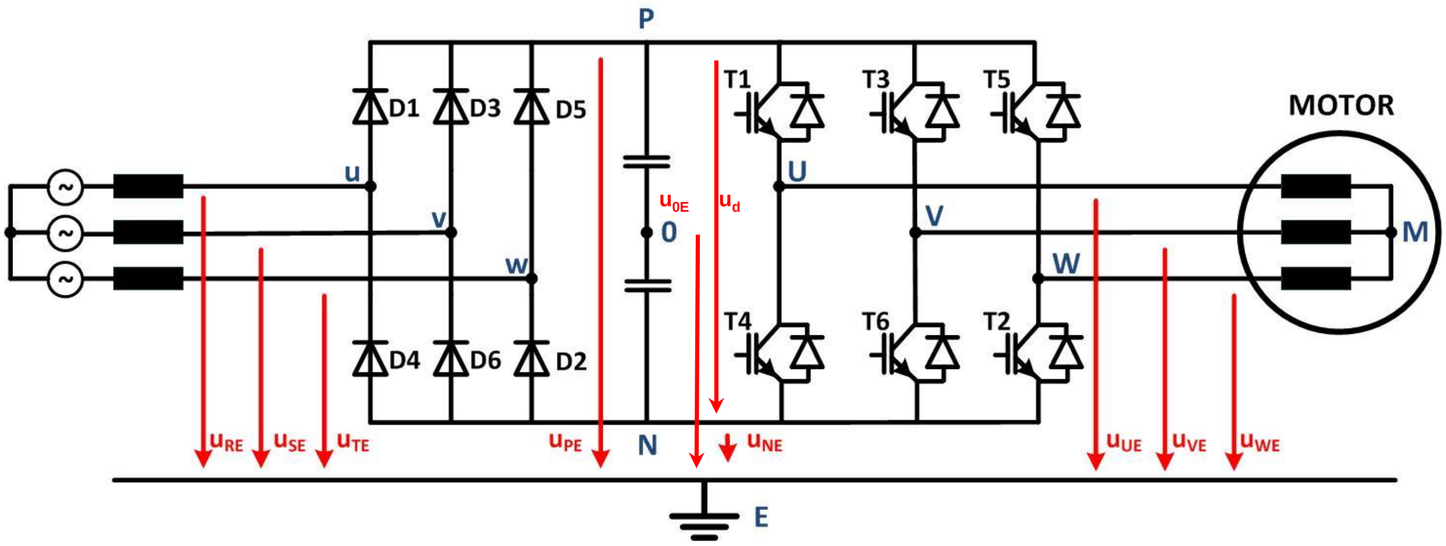

$$u_d(t) = u_{PE}(t) - u_{NE}(t) \approx const.$$

$$u_{UV}(t) = u_{UE}(t) - u_{VE}(t)$$

$$u_{CM}(t) = \frac{u_{UE}(t) + u_{VE}(t) + u_{WE}(t)}{3}$$

Side effects of motor-converter interaction

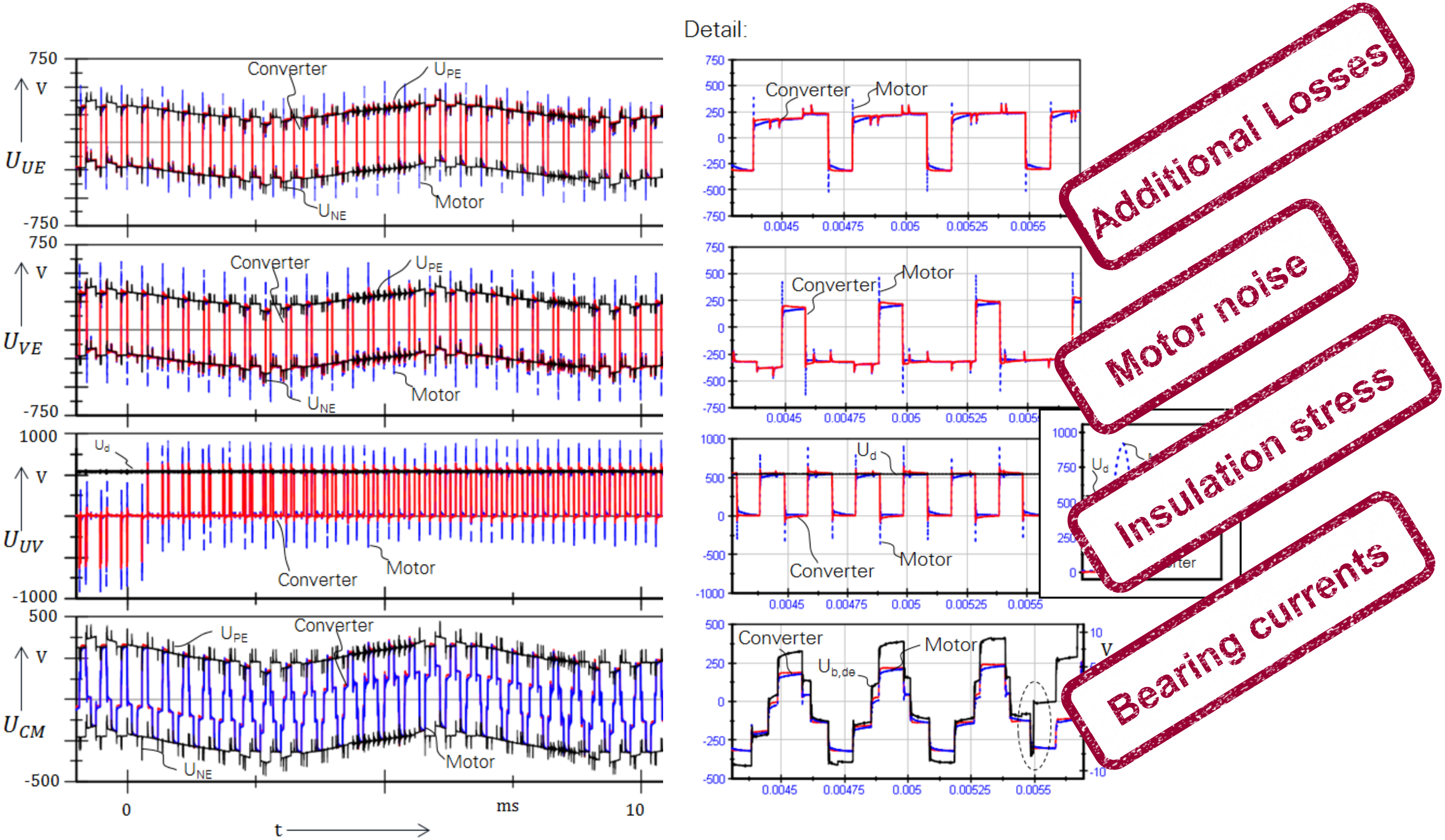

Content of chapter “Bearing currents”

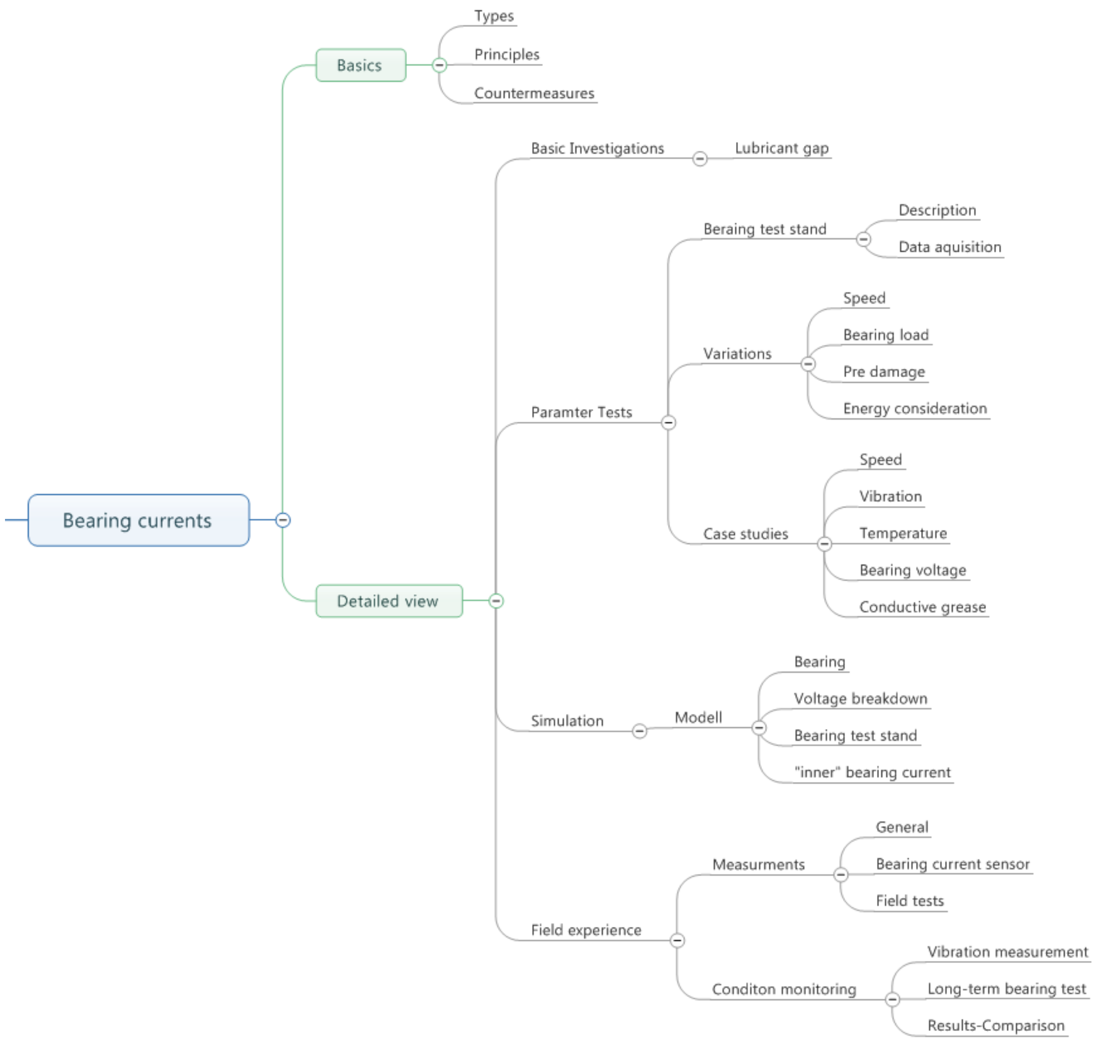

Photographs of damaged motor bearings

SIEMENS

Changes to the lubricating grease

Bearing race with matt surface

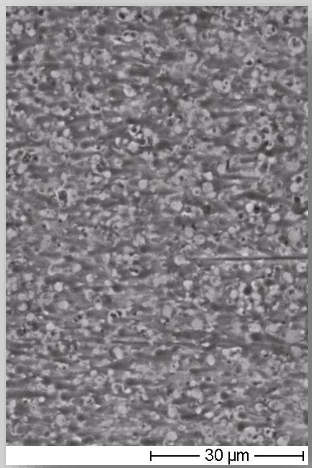

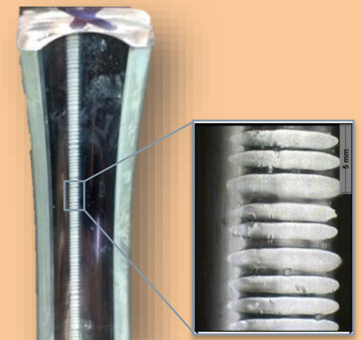

Fluted motor bearing race

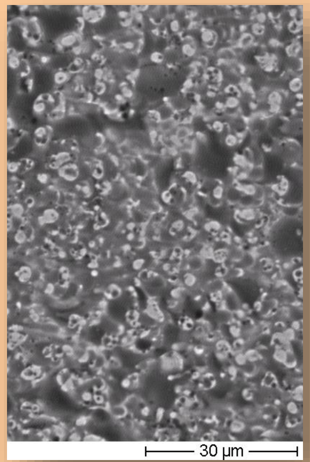

Bearing current types in the drive system

SIEMENS

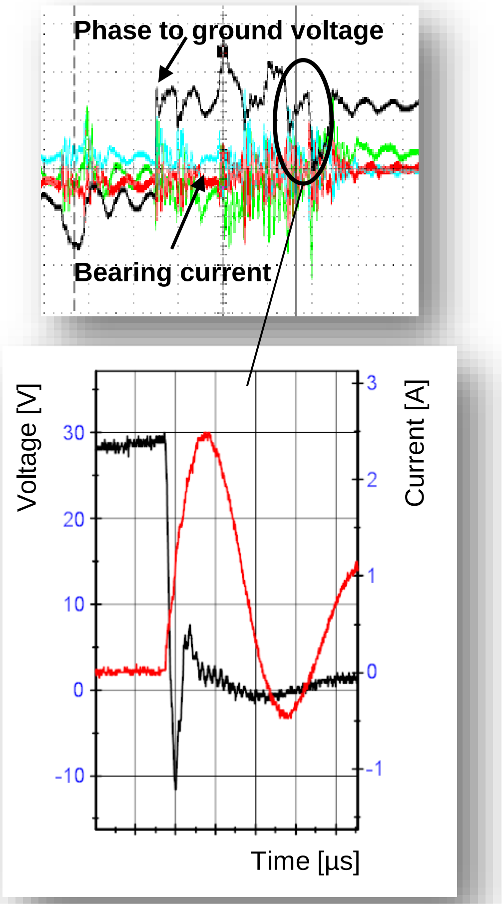

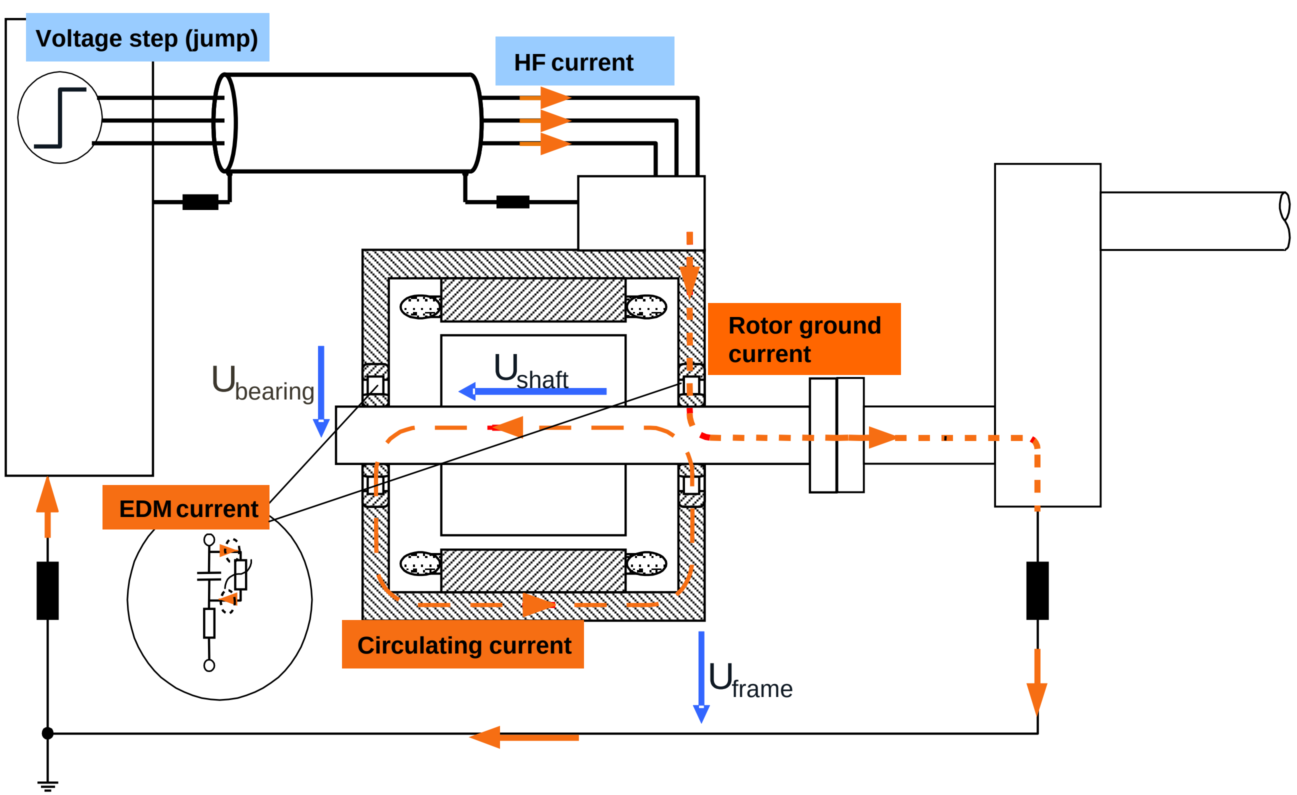

Common-mode voltage

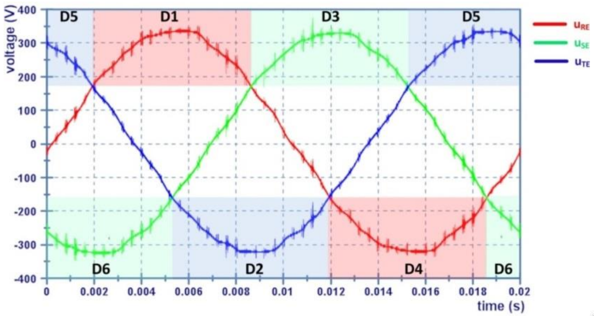

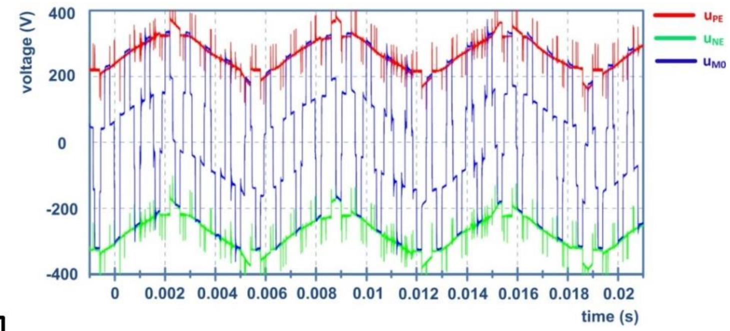

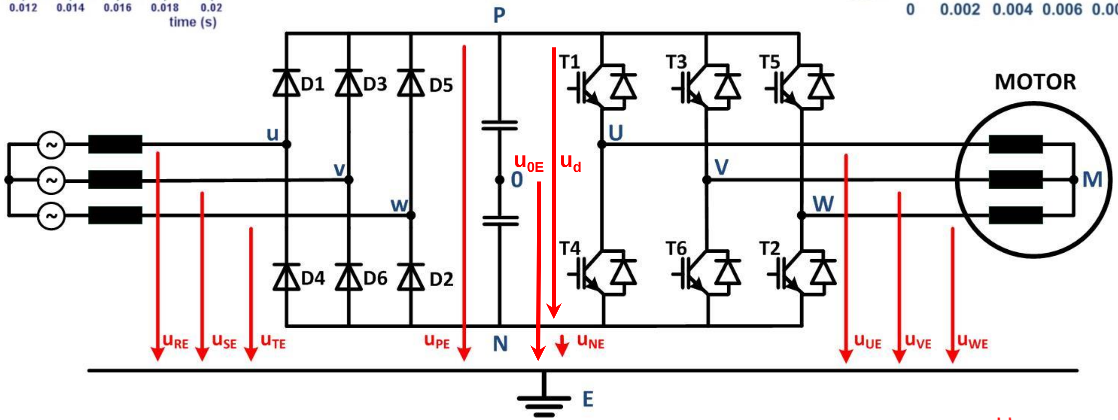

$$u_{CM}(t) = \frac{u_{UE}(t) + u_{VE}(t) + u_{WE}(t)}{3}$$

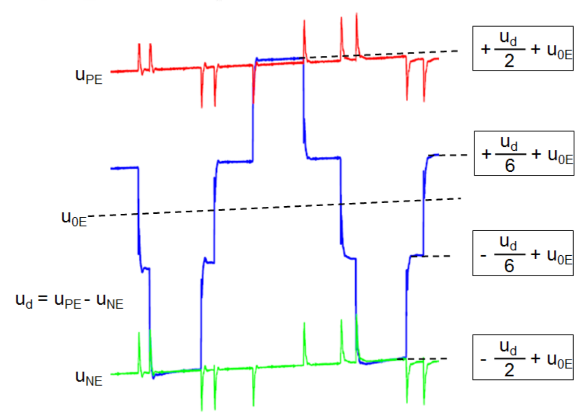

HF equivalent circuit diagram of a motor

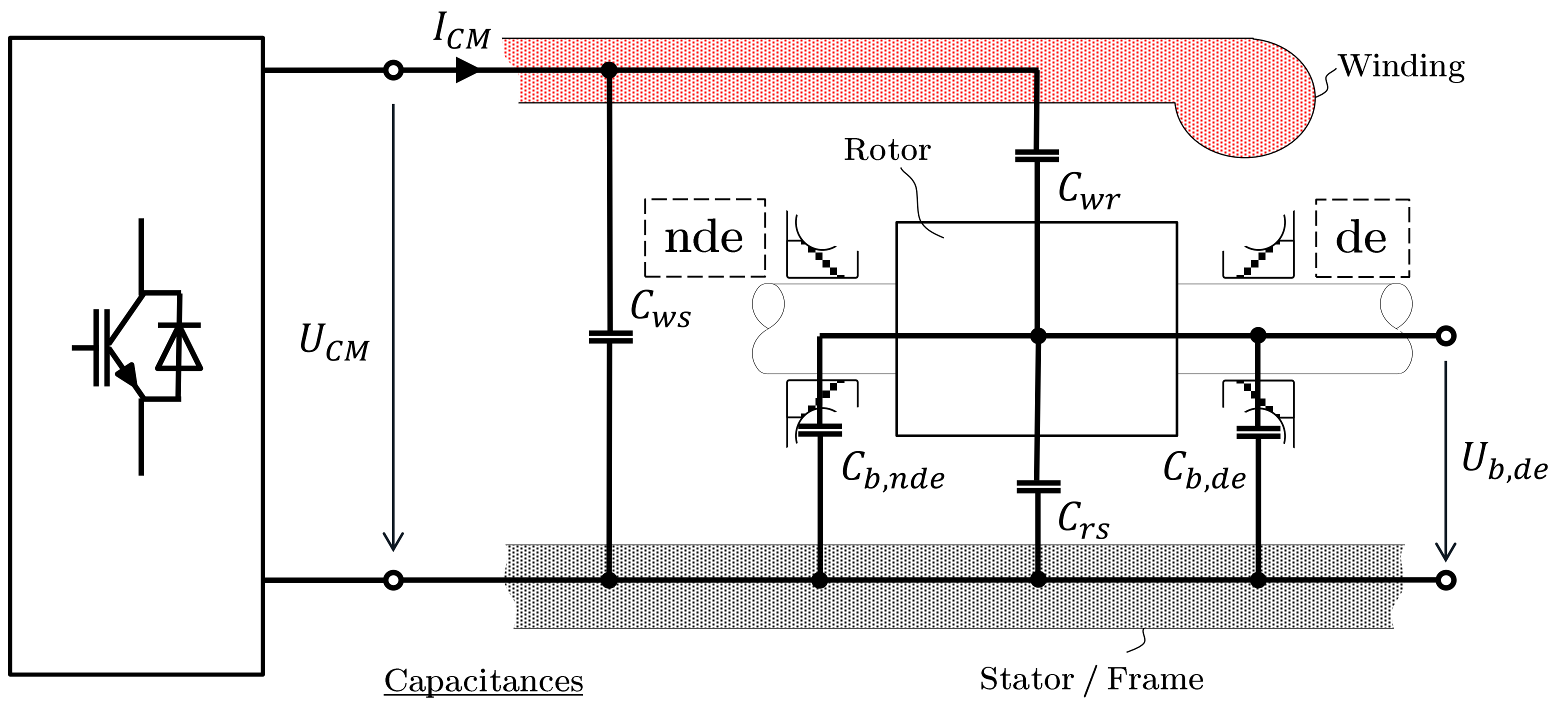

Capacitances

C_{wh}: winding––frame

C_{wr}: stator––winding

C_{rh}: rotor––stator

C_b : bearing

Bearing current type: EDM current

SIEMENS

Principle

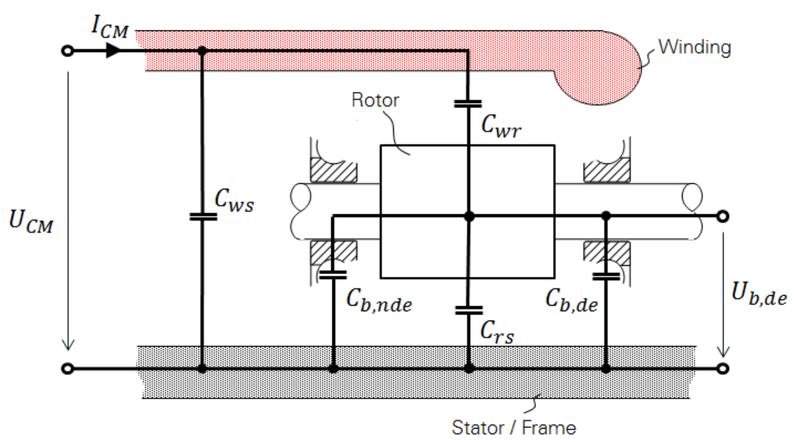

$$BVR = \frac{U_b}{U_{CM}} = \frac{C_{wr}}{C_{wr} + C_{rs} + 2 \cdot C_b}$$

Result

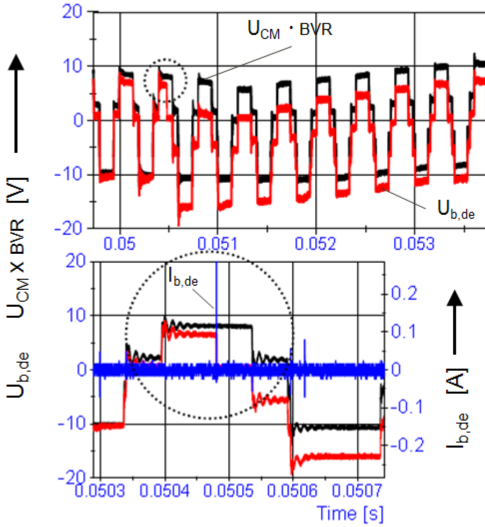

- „Transformation" of the converter common-mode voltage via BVR on the motor bearings
- Arc dicharge (EDM-currents)
- Possible initial arc for rotor ground- and circulating currents

Bearing current type: circulating current

Principle

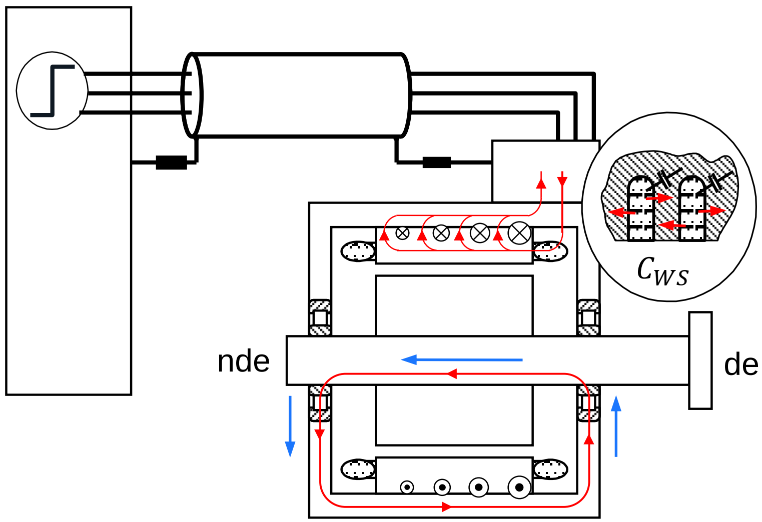

- "Leakage current" through parasitic capacitance C_{ws}
- HF circulating flux in the stator core
- Induced HF shaft voltage
- Circulating current in the shaft – bearing end shield circuit and stator core

Result & countermeasures

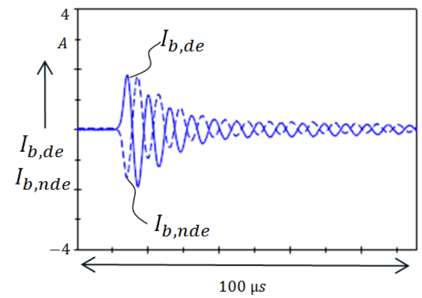

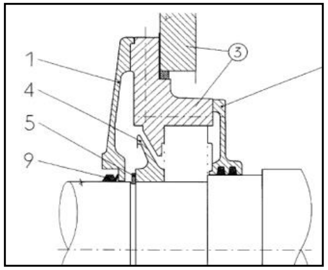

- installing an insulated bearing at the non-drive end
- insulated tachometer mounting

HF equivalent circuit diagram
A motor integrated in a drive system (1)

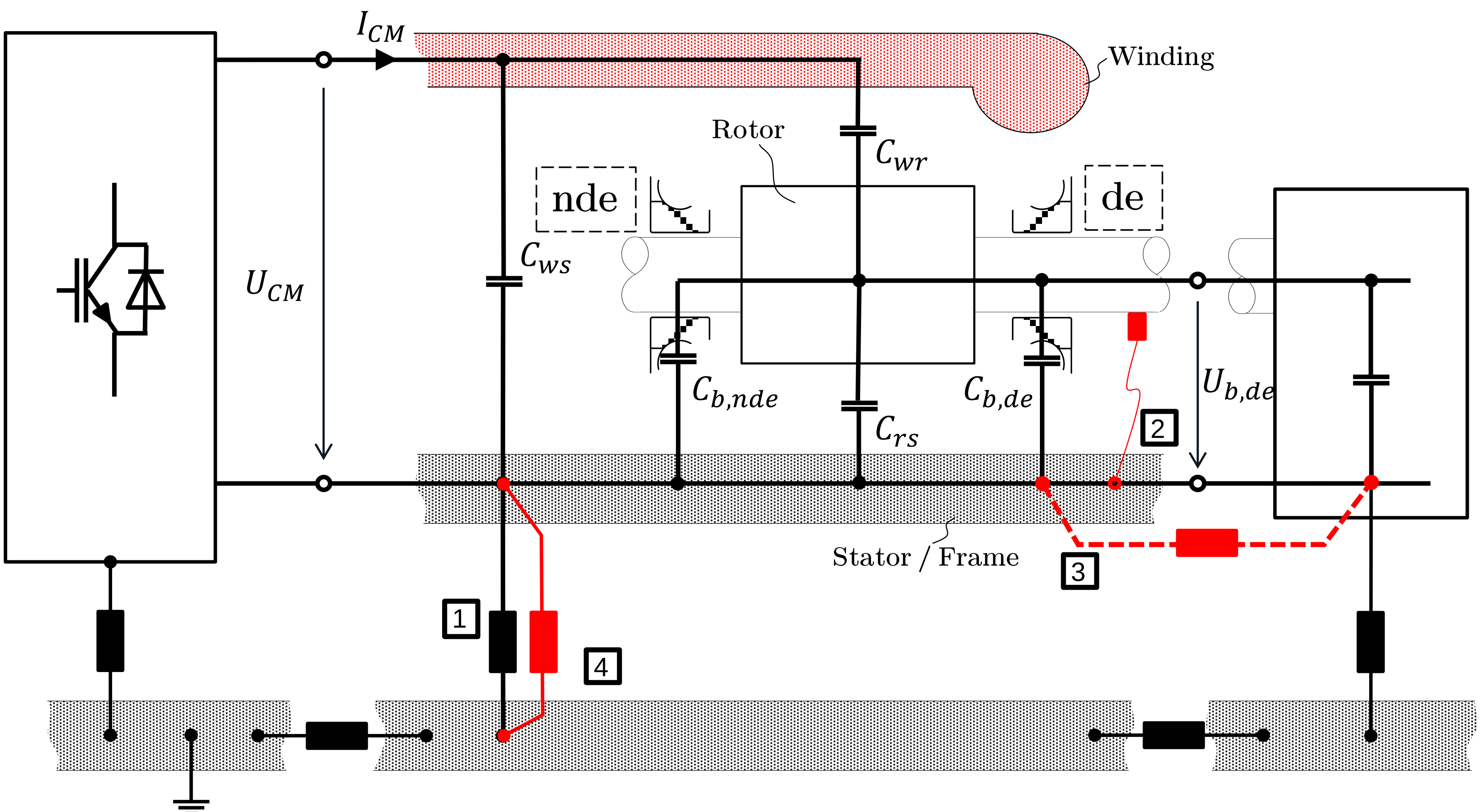

HF equivalent circuit diagram
A motor integrated in a drive system (2)

1

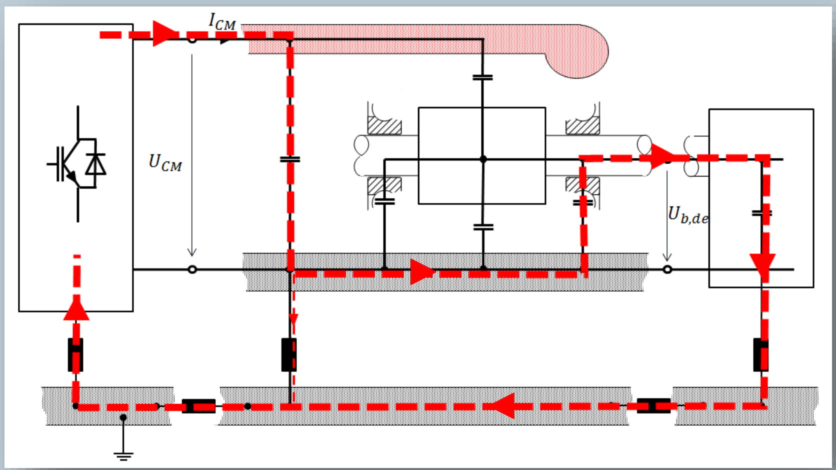

2

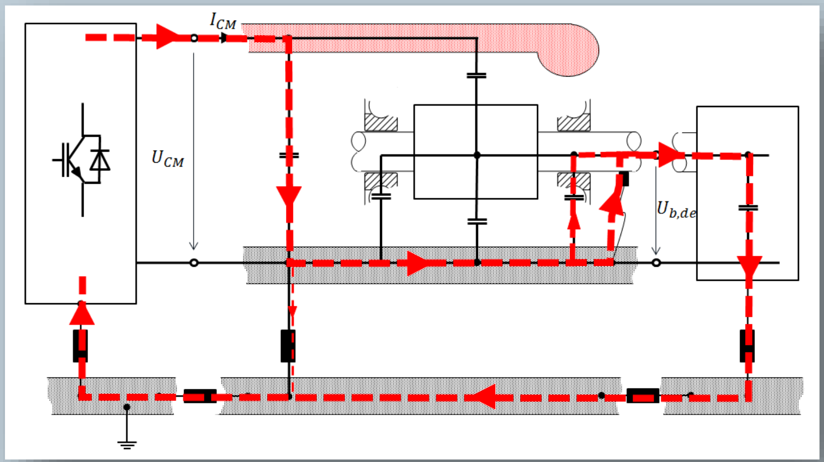

3

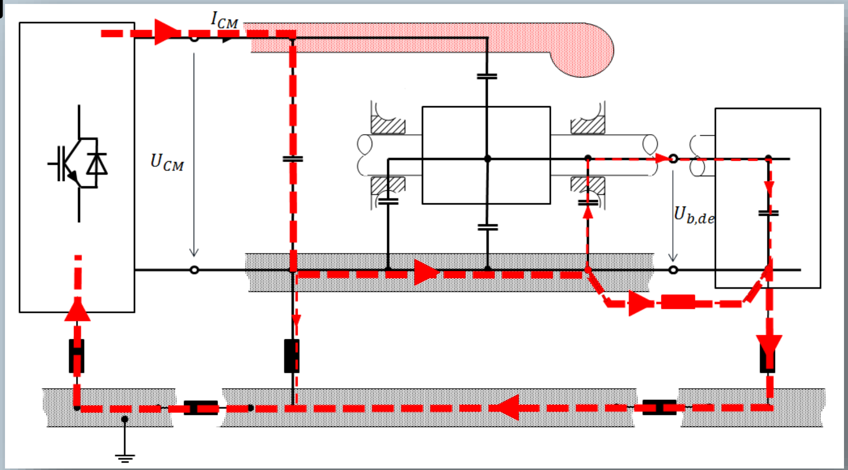

4

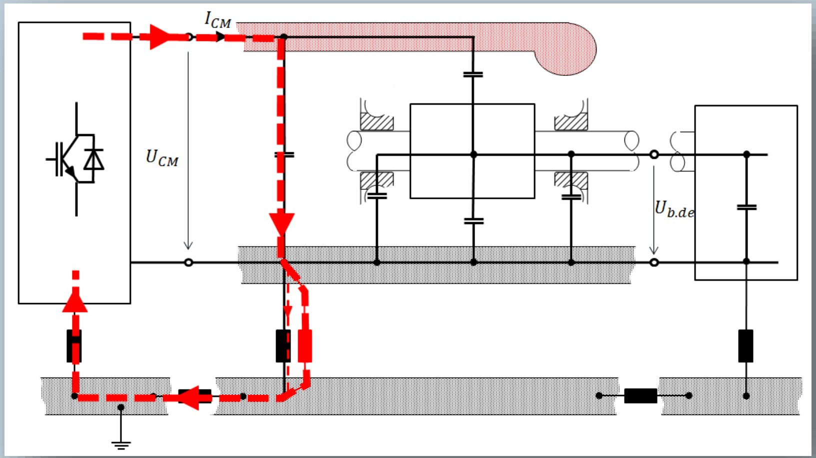

Bearing current type: rotor ground current

SIEMENS

Principle

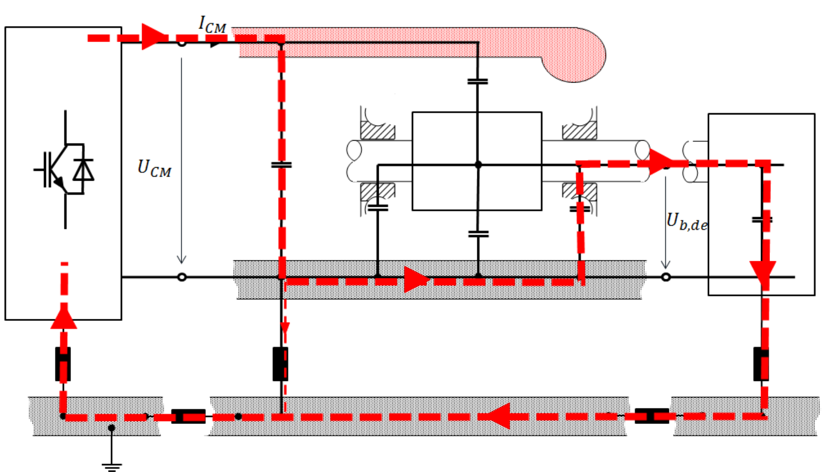

- High motor frame potential
- Good grounding on the load side
- Parasitic HF currents search for a path with the lowest resistance – through the load

Countermeasures

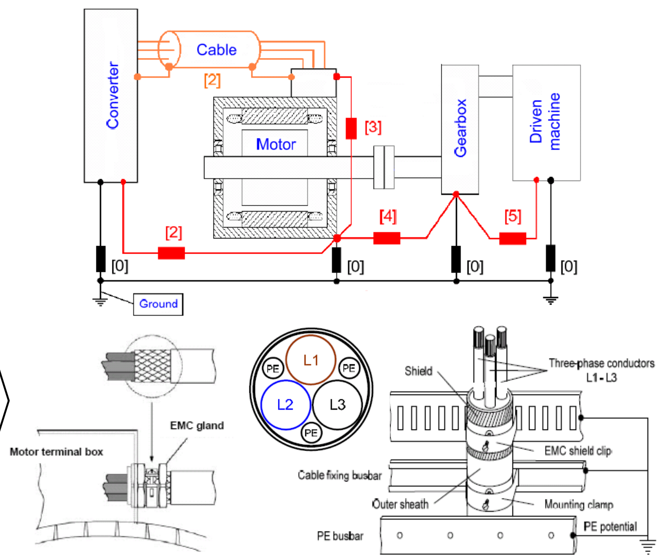

3

4

- HF grounding of the components 4
- Use symmetrically shielded motor connecting cables 4
- Potential bonding in the system 3
- Connection through the largest possible surface area 4

Using dampening cores – common mode chokes

SIEMENS

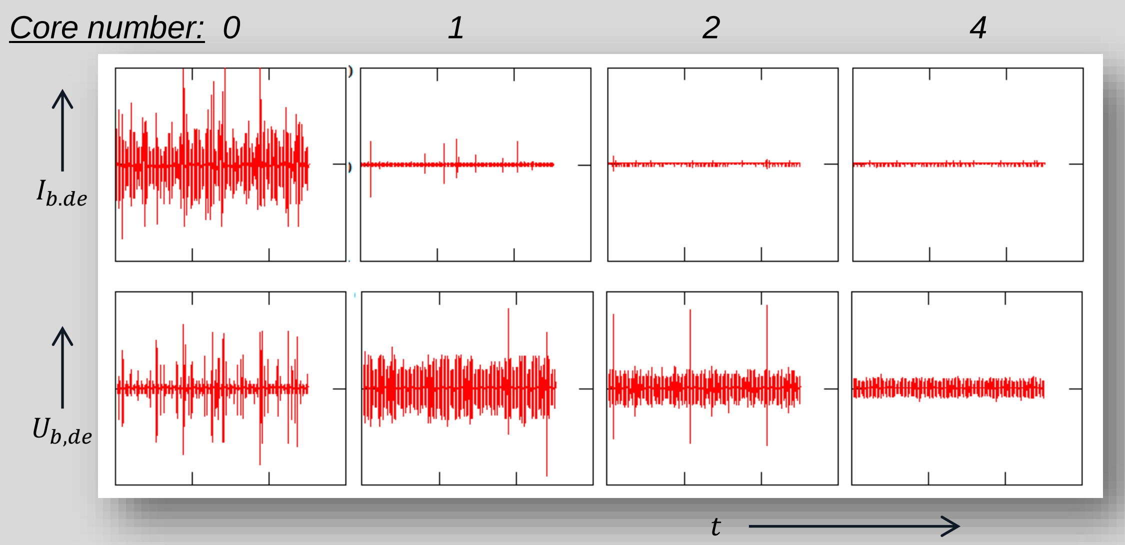

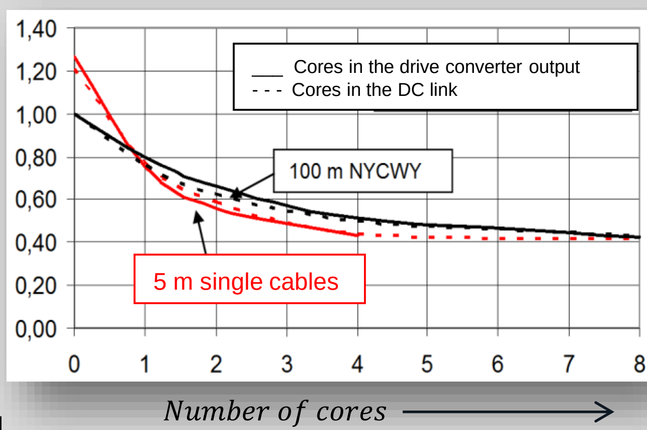

Power flow
through the bearing

- Nanocrystalline iron cores (arrangement: three phase)
- Number of cores depends on cable type, length and motor size
- EDM-currents not influenced
- Saturation in case of unbalanced connection and grounding
  → effect ⇩⇩

Distribution of the bearing current types

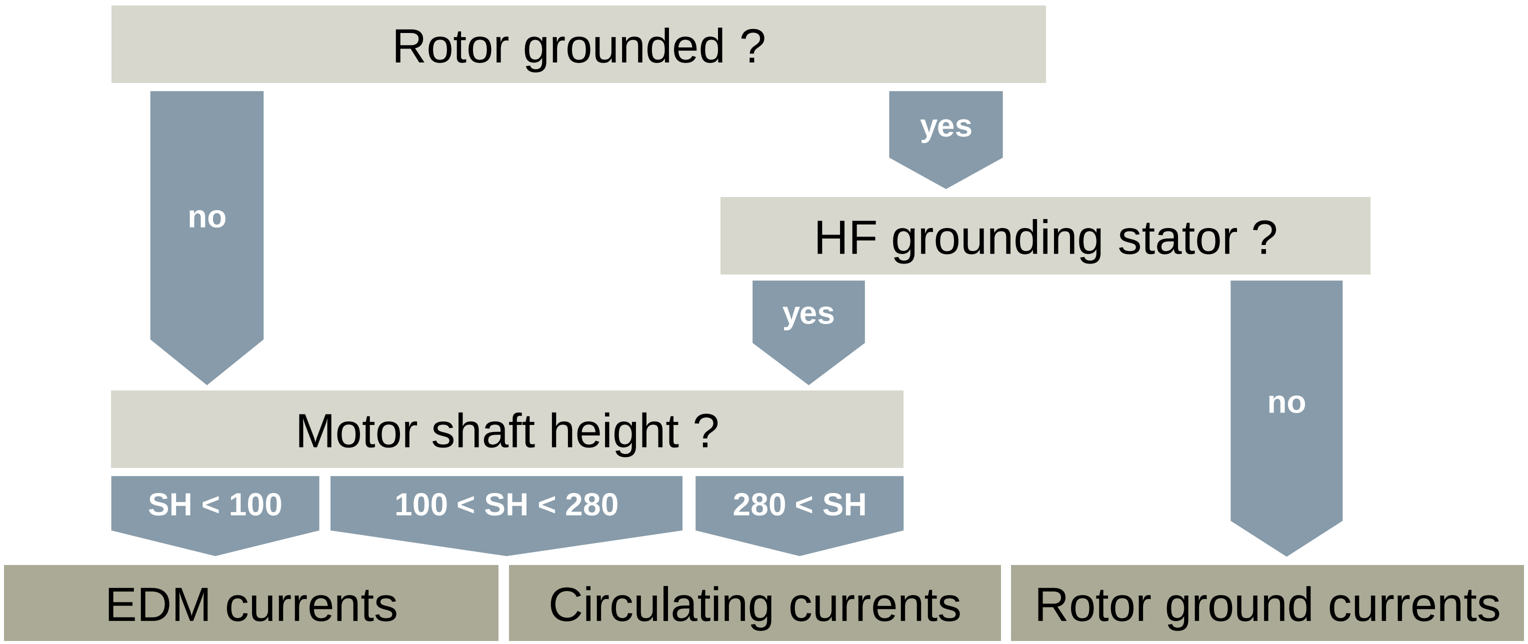

General countermeasures to reduce bearing currents

Bearing insulation

Cabling & shielding

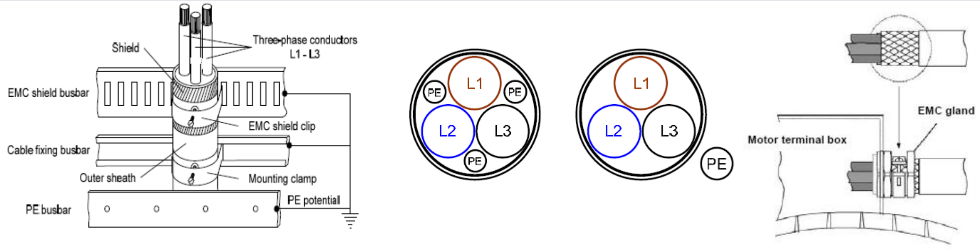

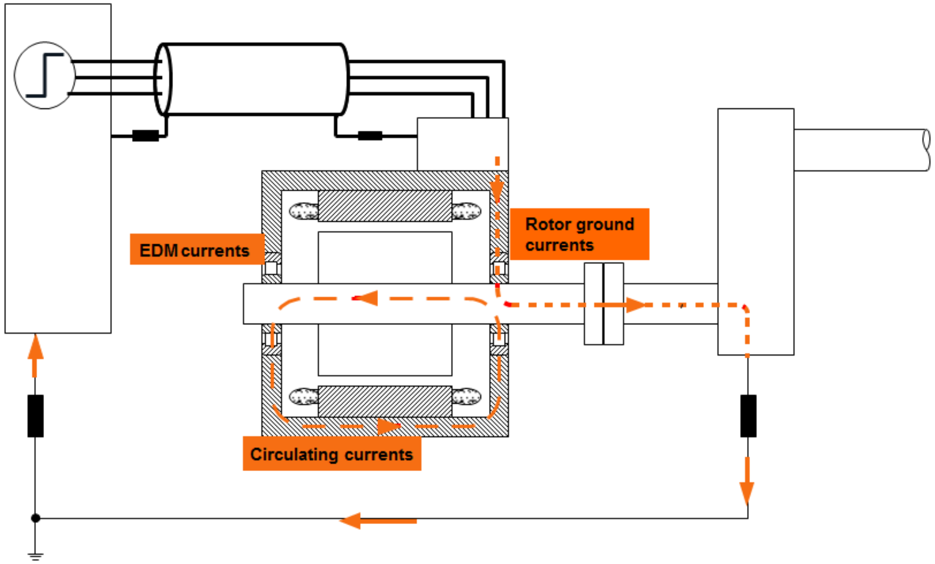

Grounding & bonding

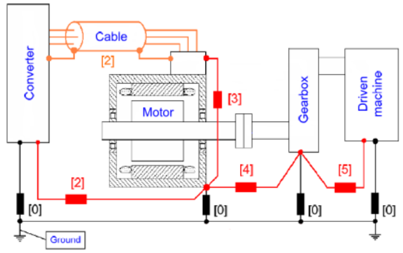

Filtering

Conclusion “Basic”-chapter

- **Bearing currents are a system issue**
- **HF current flow in the system**
  converter – motor – load – plant/system
- **Different types of bearing currents**
- **Possible corrective measures are:**
  - insulated bearing at the non-drive end
  - grounding brush
  - symmetrically-shielded connecting cables
  - shield should be connected through 360° connections
  - HF grounding and potential bonding in the system
  - good meshed plant/system grounding
  - common mode filter

Topics for a detailed investigation

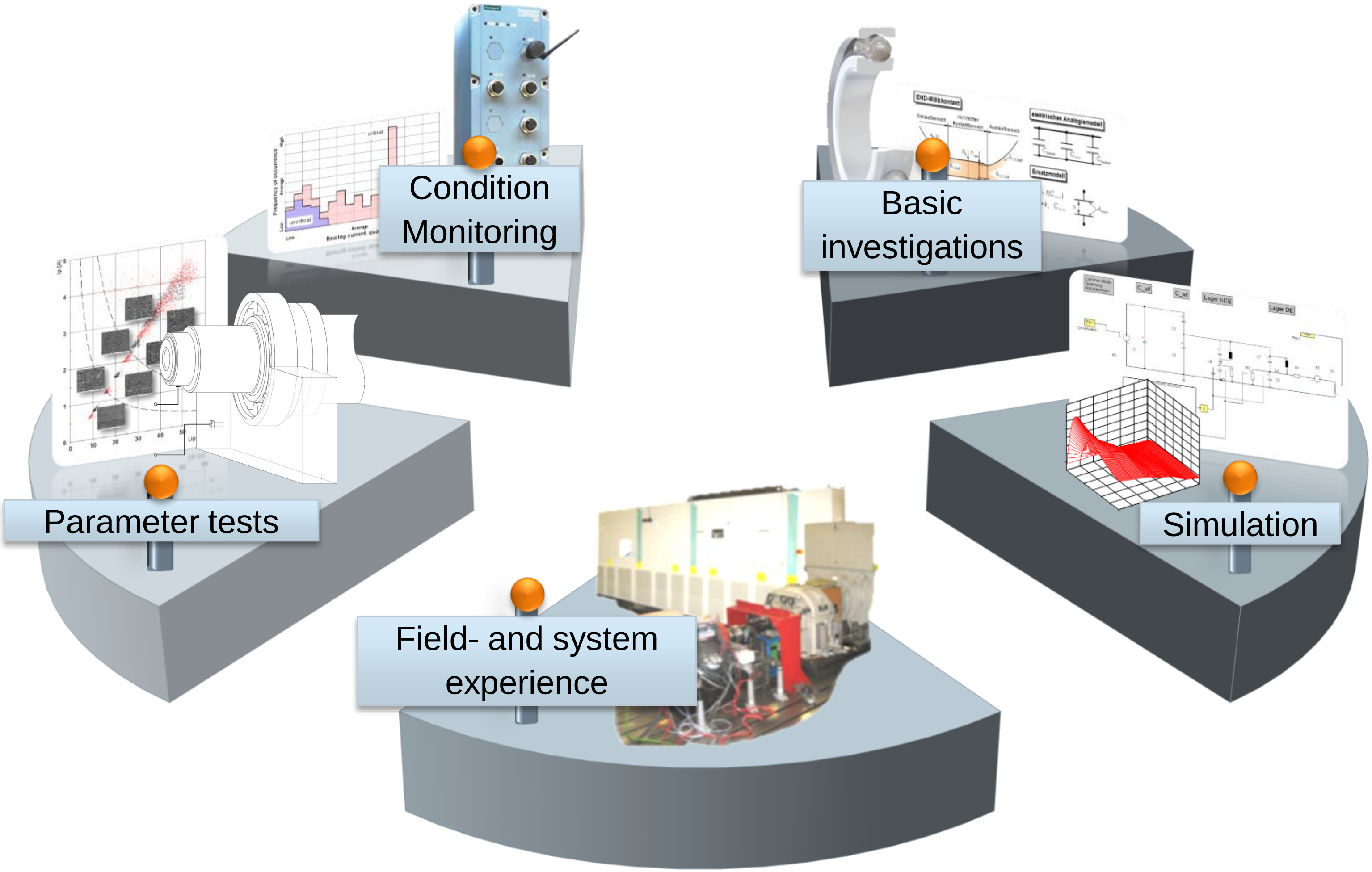

Basic investigation:
Lubricant gap and bearing model

SIEMENS

Bearing test bench for capacitance measurements

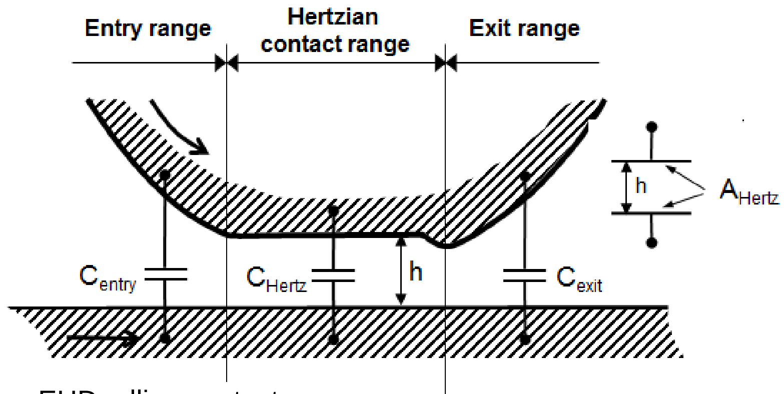

$$C_b = C_{entry} + C_{Hertz} + C_{exit}$$

$$C_b \approx k_c \cdot C_{Hertz}$$

EHD rolling contact

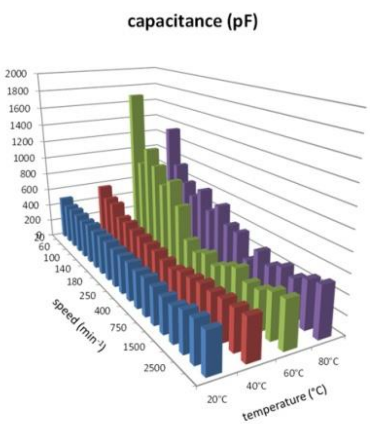

Measured capacitances

$$C(n) = a + b \cdot n + c \cdot n^d$$

$$h = \frac{k_C \cdot \varepsilon_0 \cdot \varepsilon_r \cdot A_{Hertz}}{C_b}$$

$$CP(n) = a + b \cdot n + c \cdot (1 - e^{\frac{-n}{d}})$$

$$CP = \frac{\hat{U}_b}{\hat{U}_0} \cdot 100\%$$

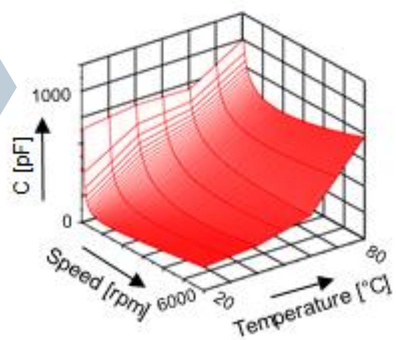

Bearing capacitance

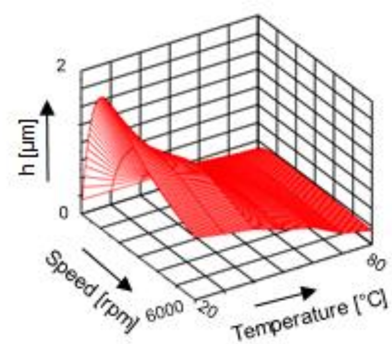

Lubricant gap

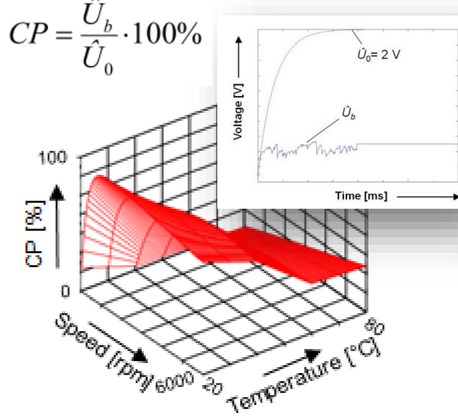

Capacitance probability

Parameter tests:
Description of the bearing current test stand

- Closed-loop controlled operation
- Continuous data logging
- Variation of mech. and elec. parameters
  - → Voltage (current)
  - → Pulse frequency
  - → Speed
  - → Temperature
  - → Vibration
  - → Bearing load

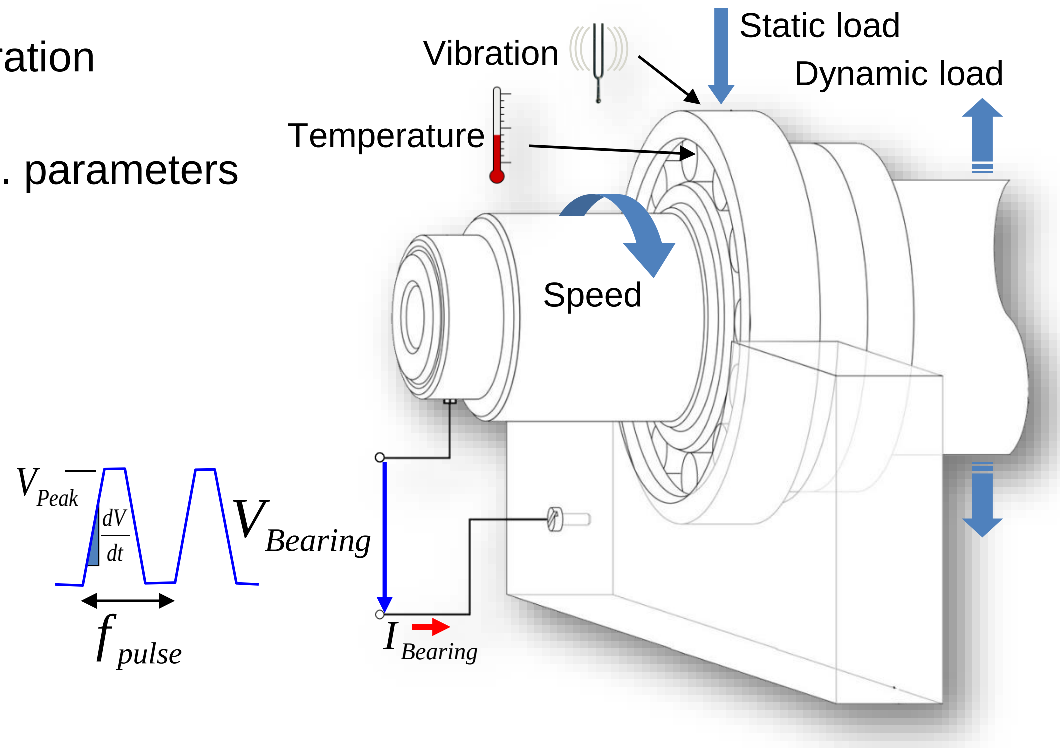

Electric load states

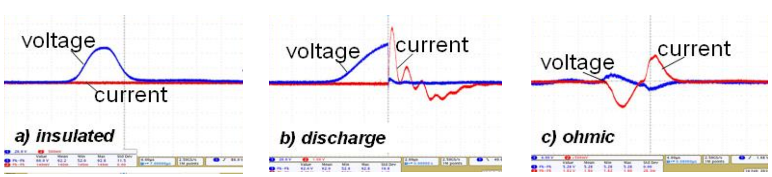

Parameter tests:
Data acquisition and evaluation

SIEMENS

(1) 1s- plot: peak value sorting

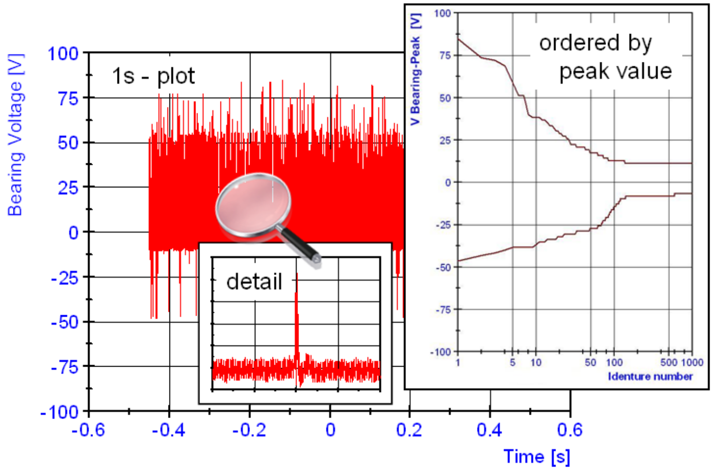

(3) Vibration measurements and FFT

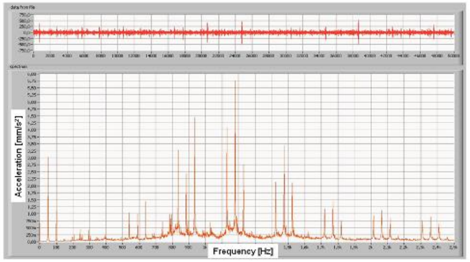

(2) 1µs- plot: energy method

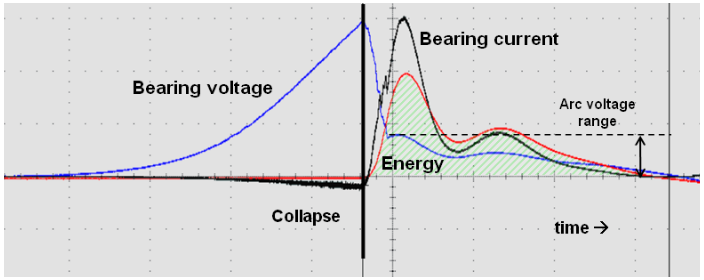

(4) Scanning electron microscope (SEM)

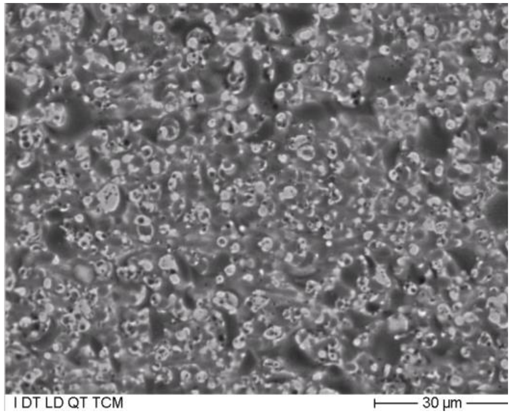

SIEMENS

5-hour test – speed variation

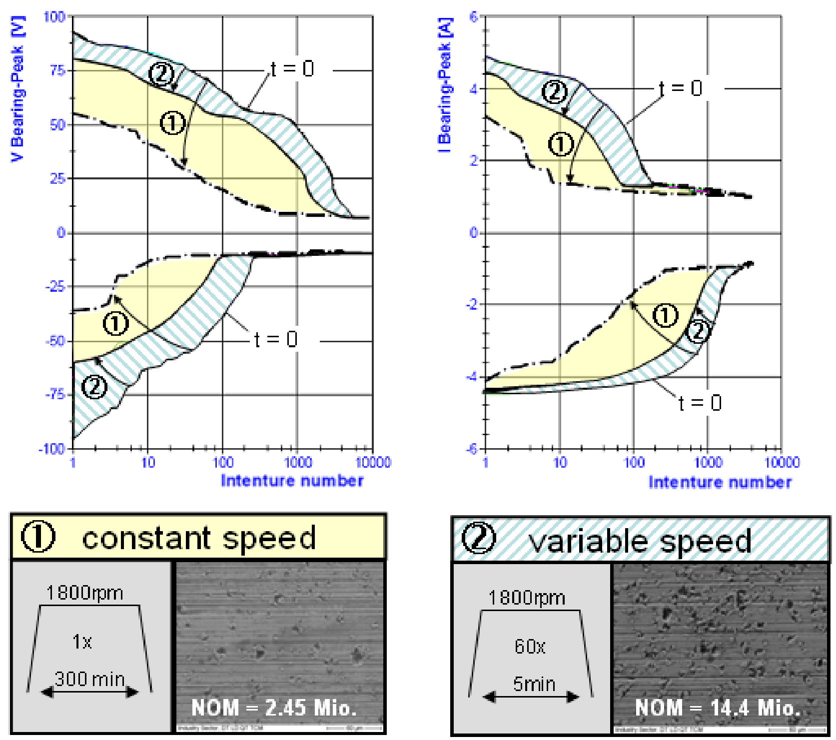

NOM: Numbers of Meltingpoints

- Variable-speed operation increases the maximums of voltage peaks at the bearing just as a result of the variation in speed alone.

Parameter tests:
Reproducible corrugation tests

Influence of the bearing load

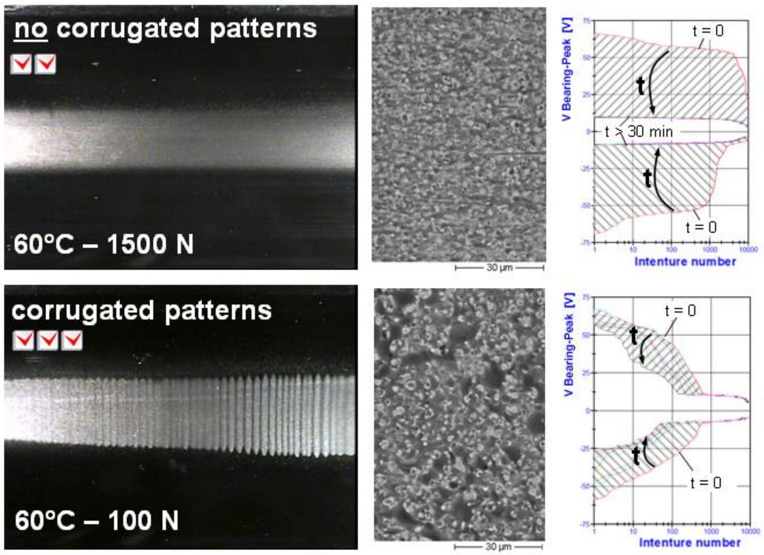

3000rpm const. , $V_{bearing, max.}$= 70V_p, f_{pulse} = 2,5kHz, T_{rise}=5ns T_{width}=5µs

- Reproducible corrugation tests are possible
- A bearing operated with increased underload condition is more prone to corrugation.

Influence of predamage

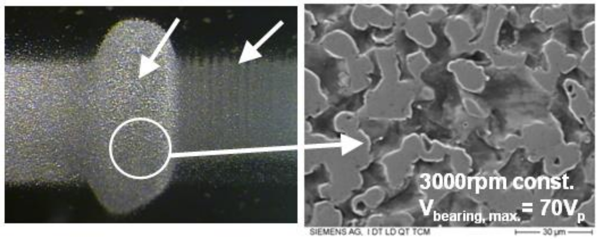

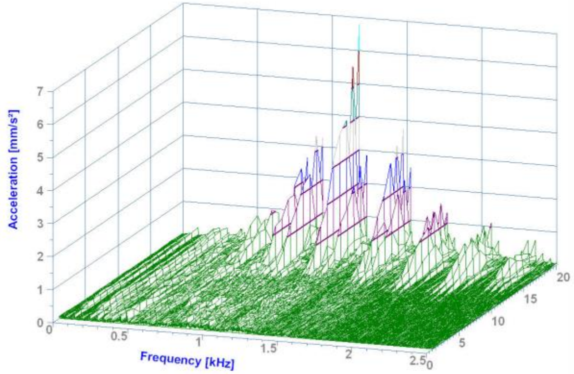

- A predamaged bearing with is more prone to corrugation.

Parameter tests:
Energy consideration

SIEMENS

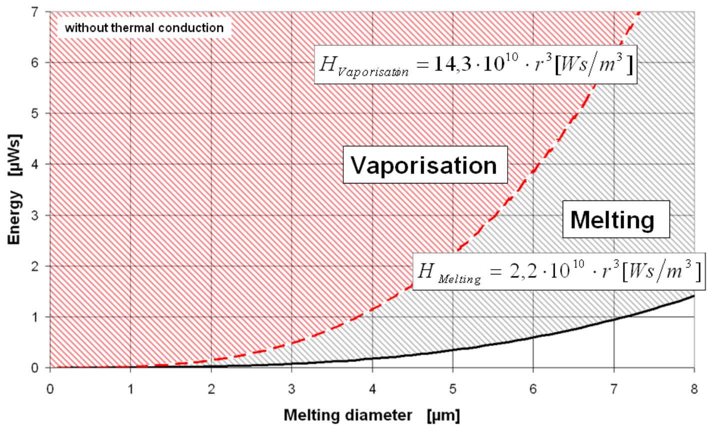

Energies from <u>enthalpy consideration</u>

- Calculated melting and vaporization energy levels with respect to the crater diameter
- Melting and vaporization of a simplified approximated hemisphere volume
- Without thermal conduction

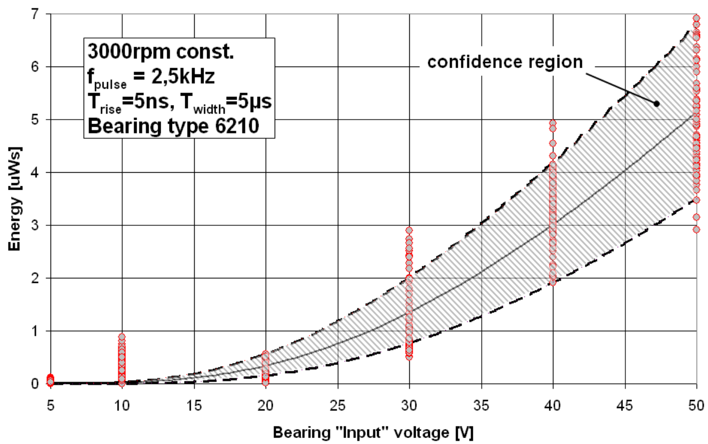

<u>Measured</u> energies vs. bearing voltage

- Bearing input voltage represents the max. value that the bearing voltage can reach at the moment of collapse
- The scatter band represents the real voltage and energy levels

- In addition to the bearing voltage, the energy absorbed in the lubricant gap is also decisive for corrugation.
- Possible limit values can be defined using the material vaporization approach

Parameter tests: Case study – speed dependency

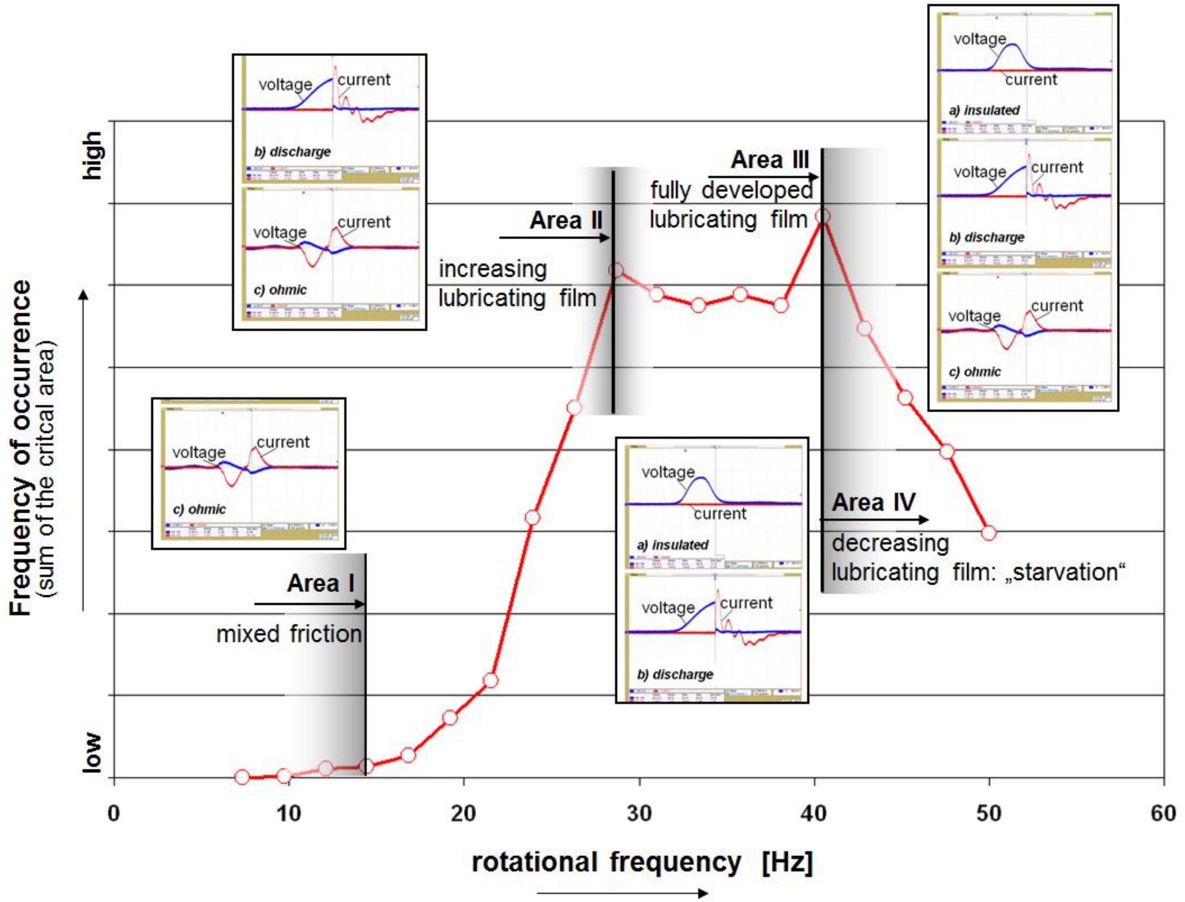

- Influence of lubrication and friction status in the bearing
- Rotational speed has a significant influence on the number of bearing current events

Parameter tests:
Case study – influence of vibration

Bearing voltage

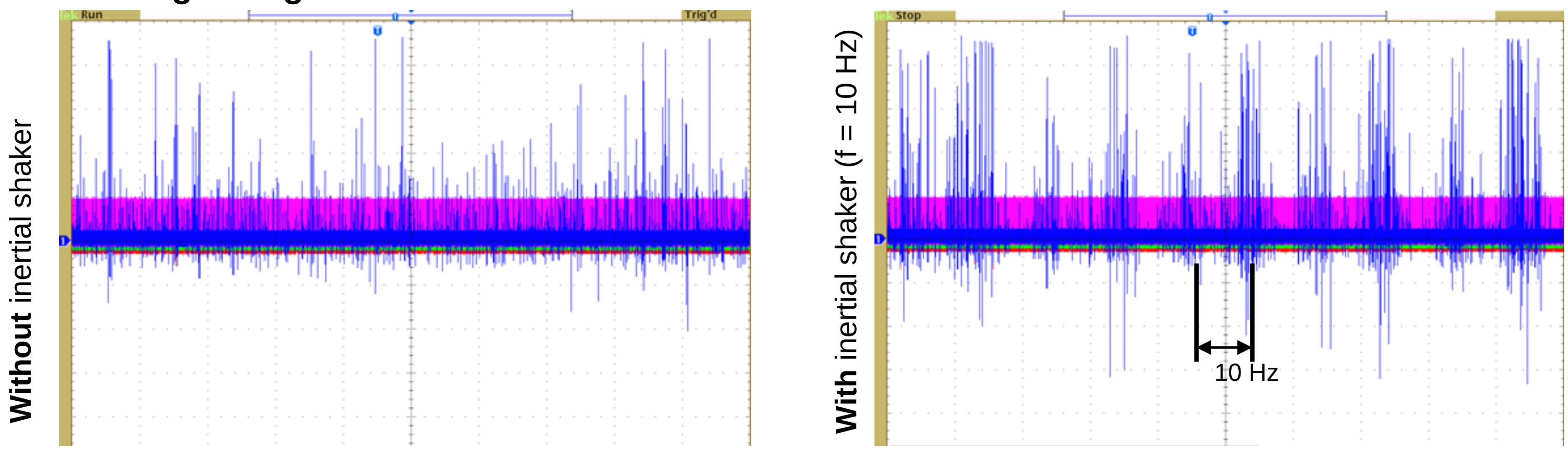

- The frequency of occurrence of voltage breakdowns in the lubricant gap followed by electric arcing depends on the status of the mechanical load. In this case, the vibration frequency and the vibration level are important influencing quantities.

Parameter tests:
Case study – influence of bearing temperature

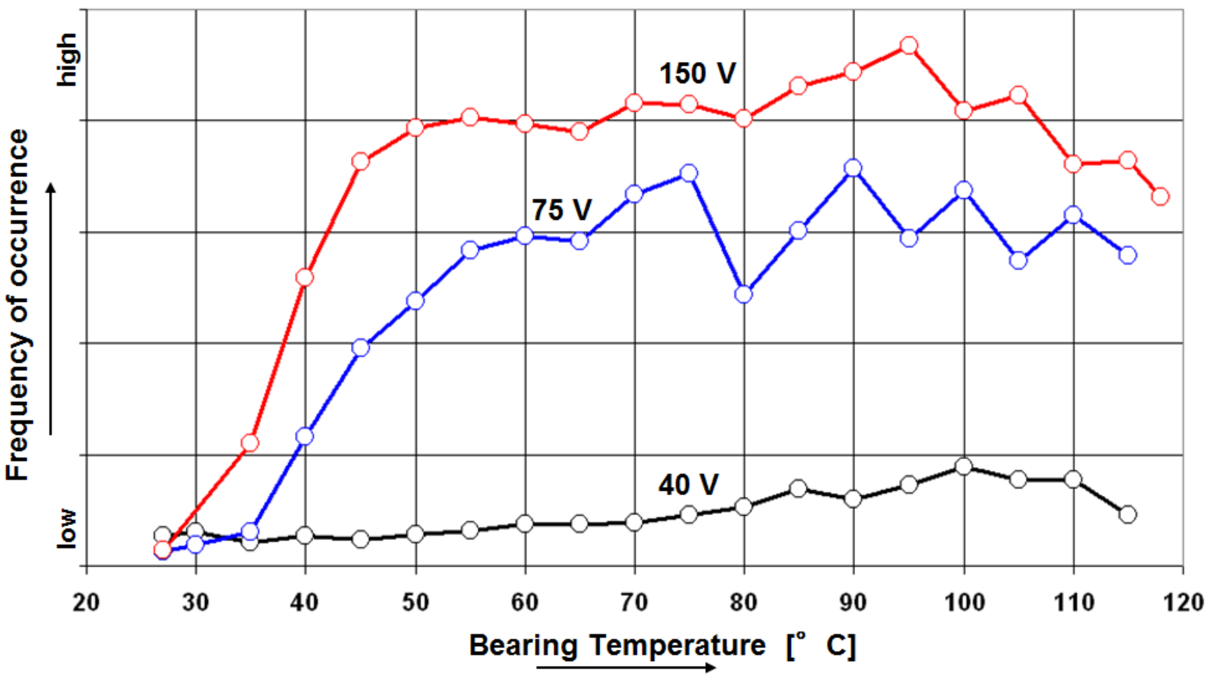

- In addition to the bearing voltage, the bearing temperature is also an important parameter that influences the frequency of bearing current events

Parameter tests:
Case study – influence of bearing voltage

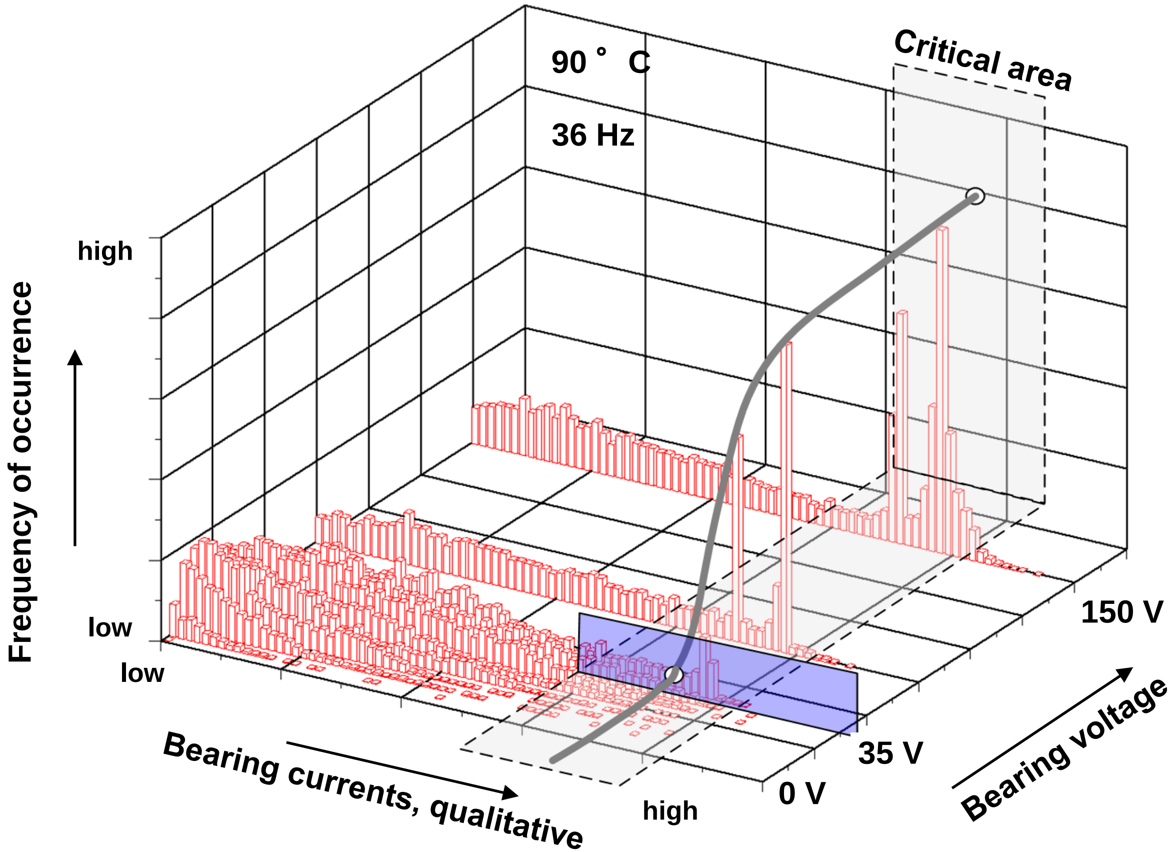

- Increase of bearing current events in the critical area above 35 V
- Under these test conditions, the limit value of 30 kV/mm was reached at the bearing voltage of 35 V

Parameter tests:
Case study – conductive grease

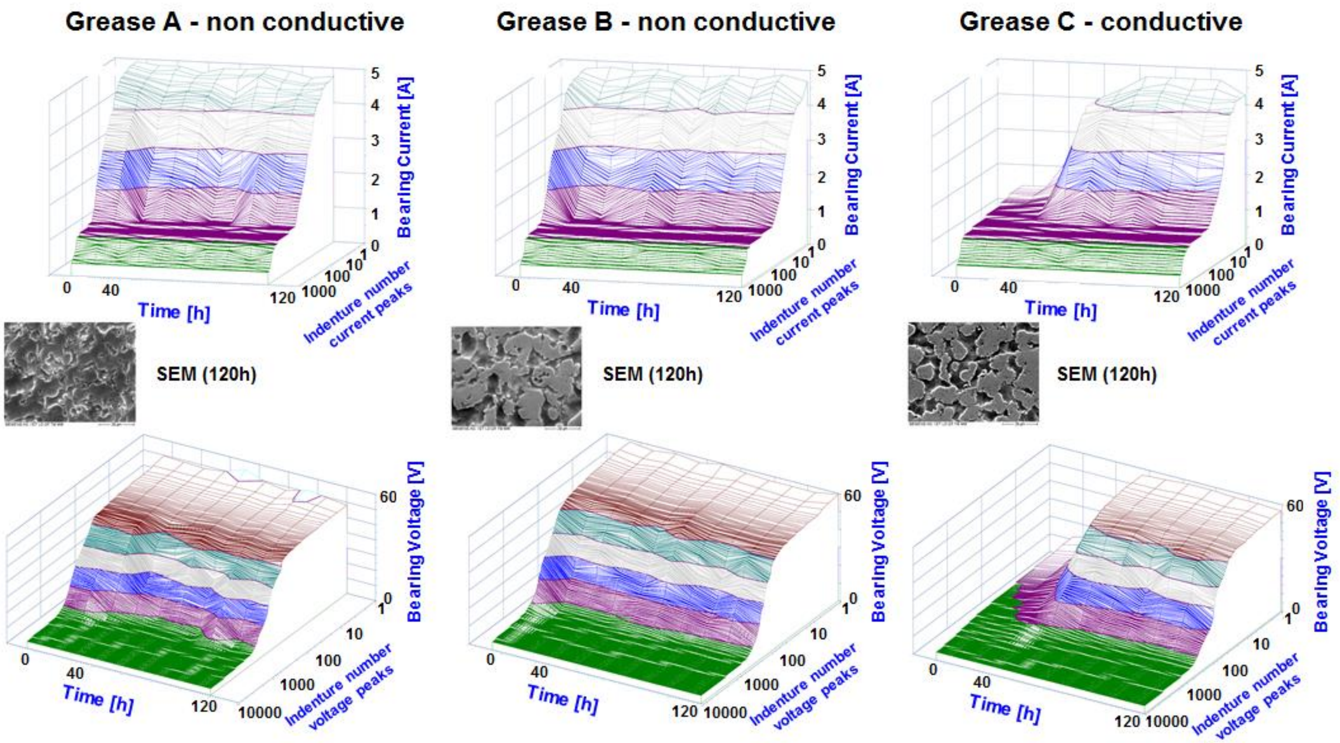

- The conductive grease being evaluated loses its electrical conductivity after a test time of 40 h
- After this time the electrical behavior of the conductive grease is comparable with typical non-conductive grease

Possible electric load states

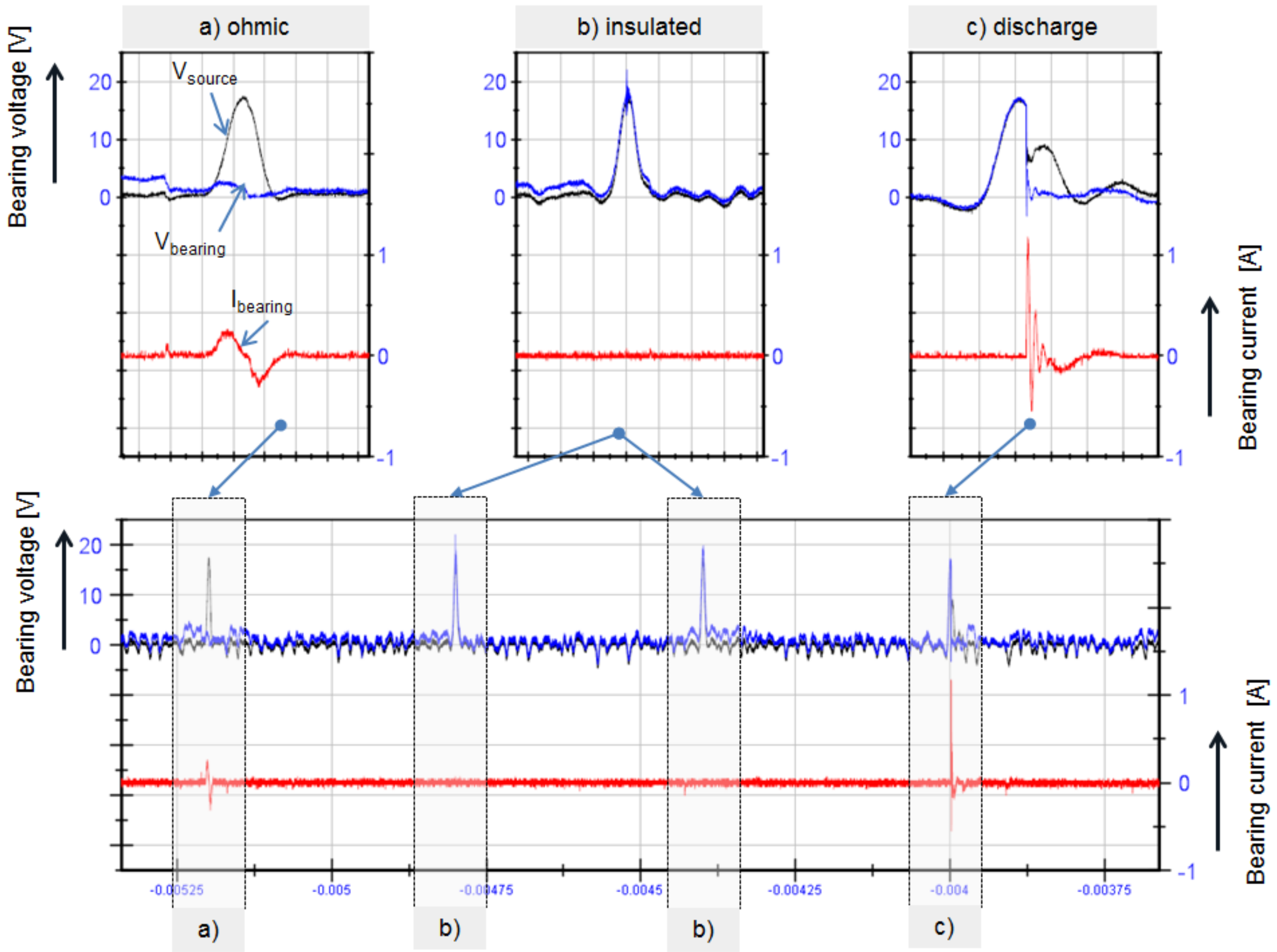

Simulation:
Electrical bearing model

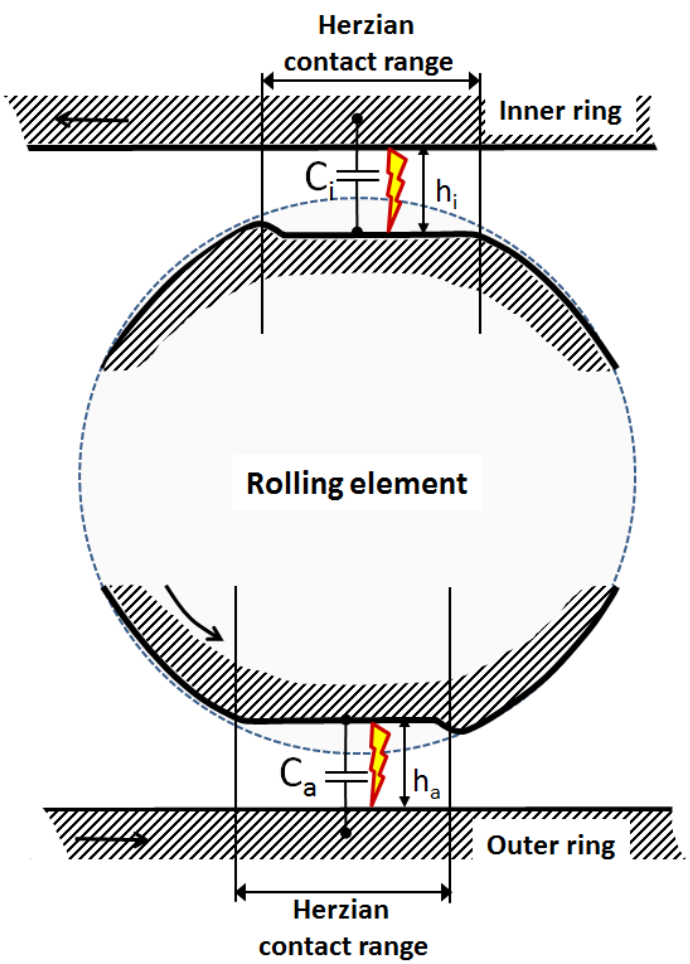

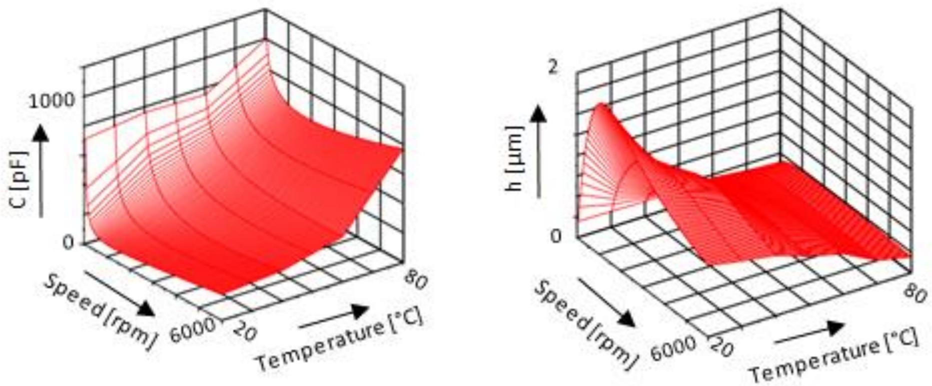

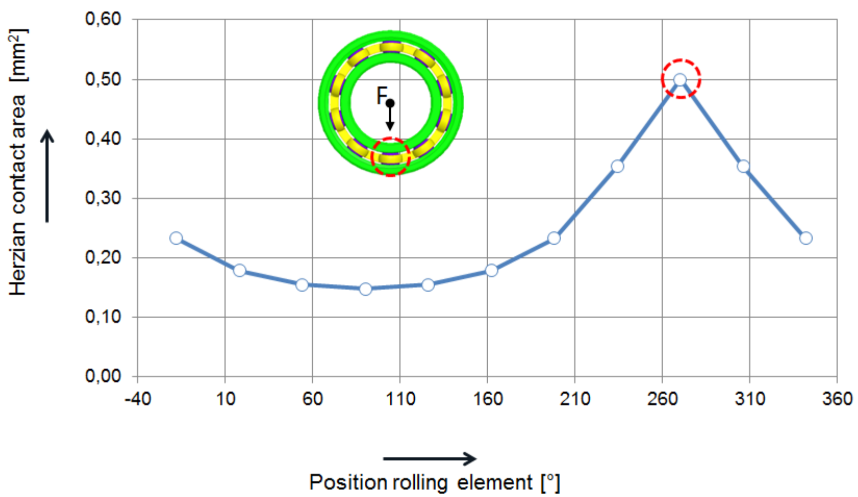

Simulation:
Voltage breakdown

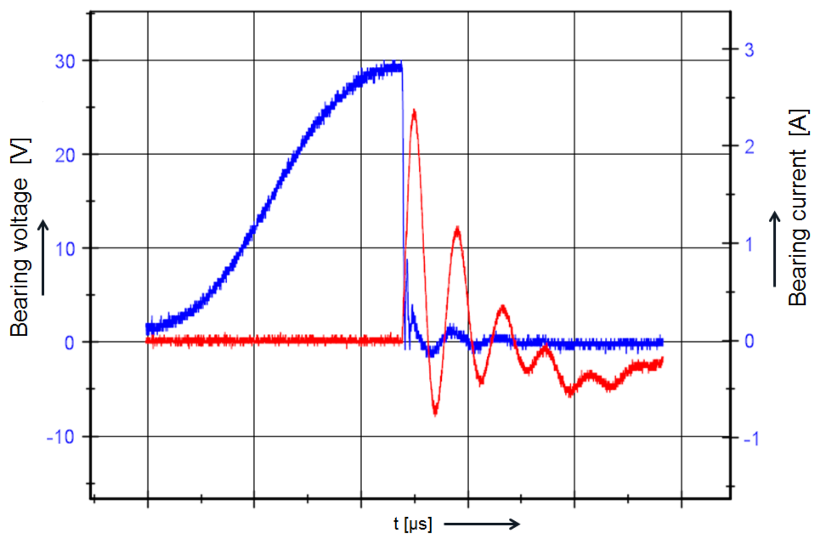

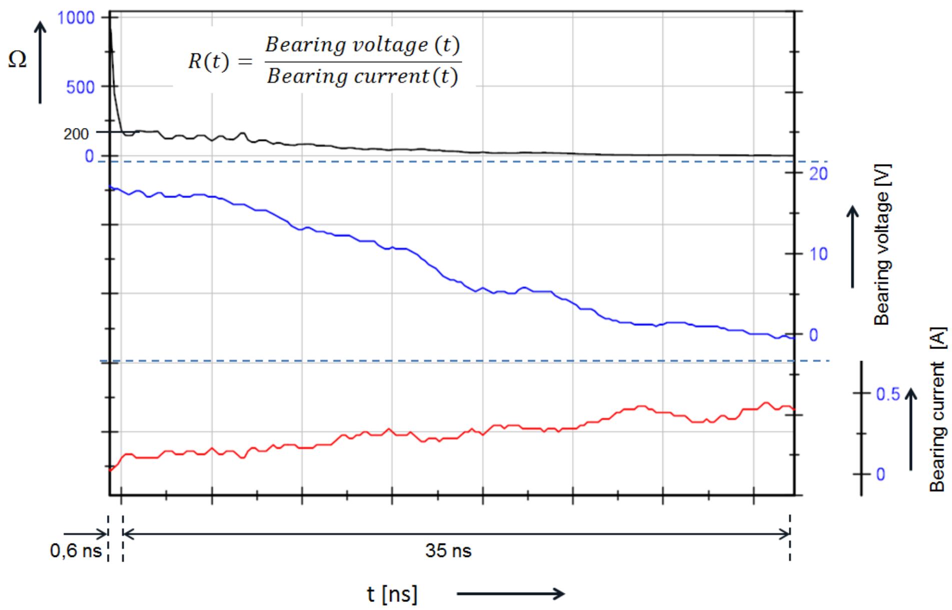

Simulation:
Bearing test stand model

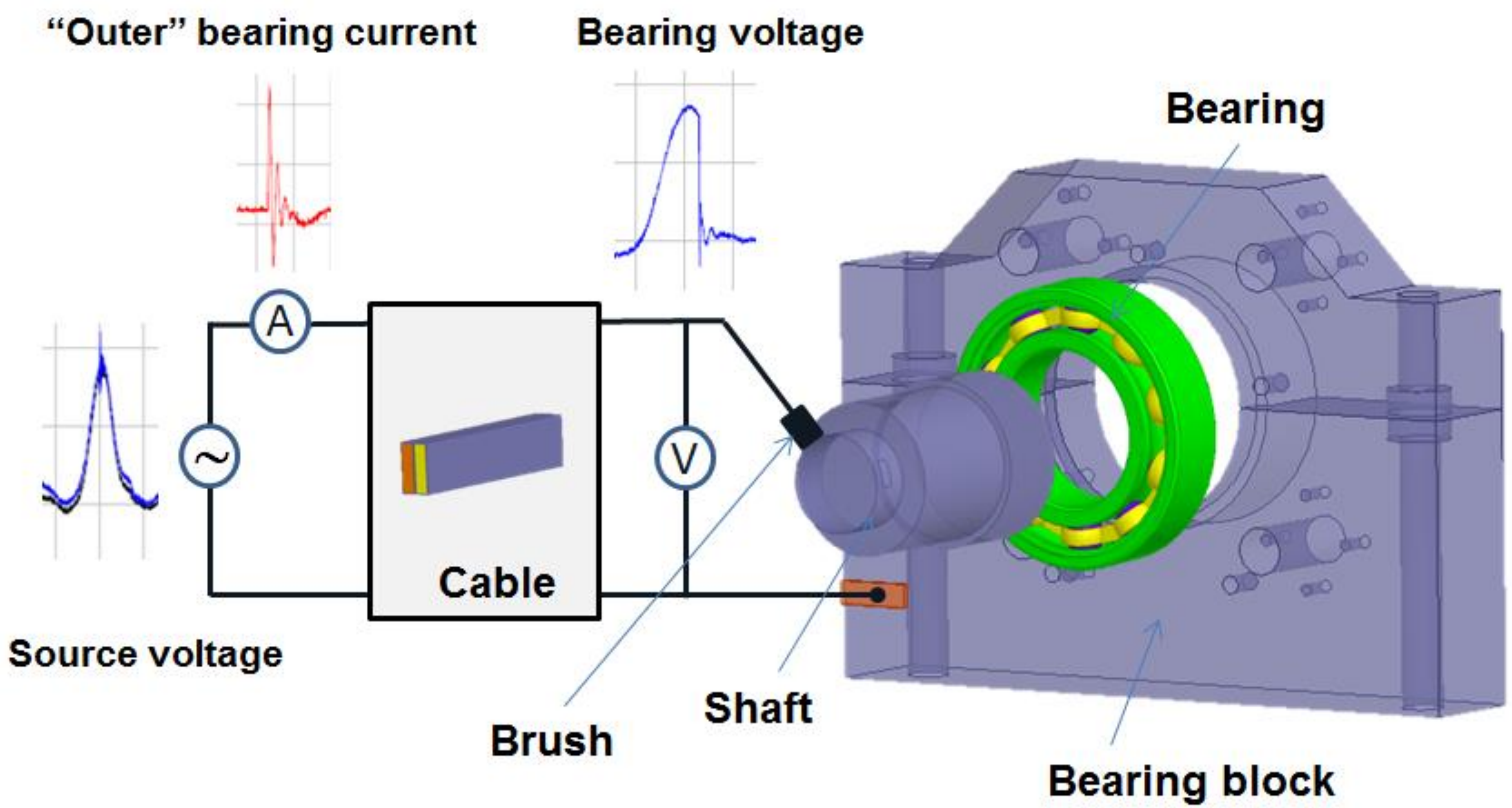

Simulation: Overall model

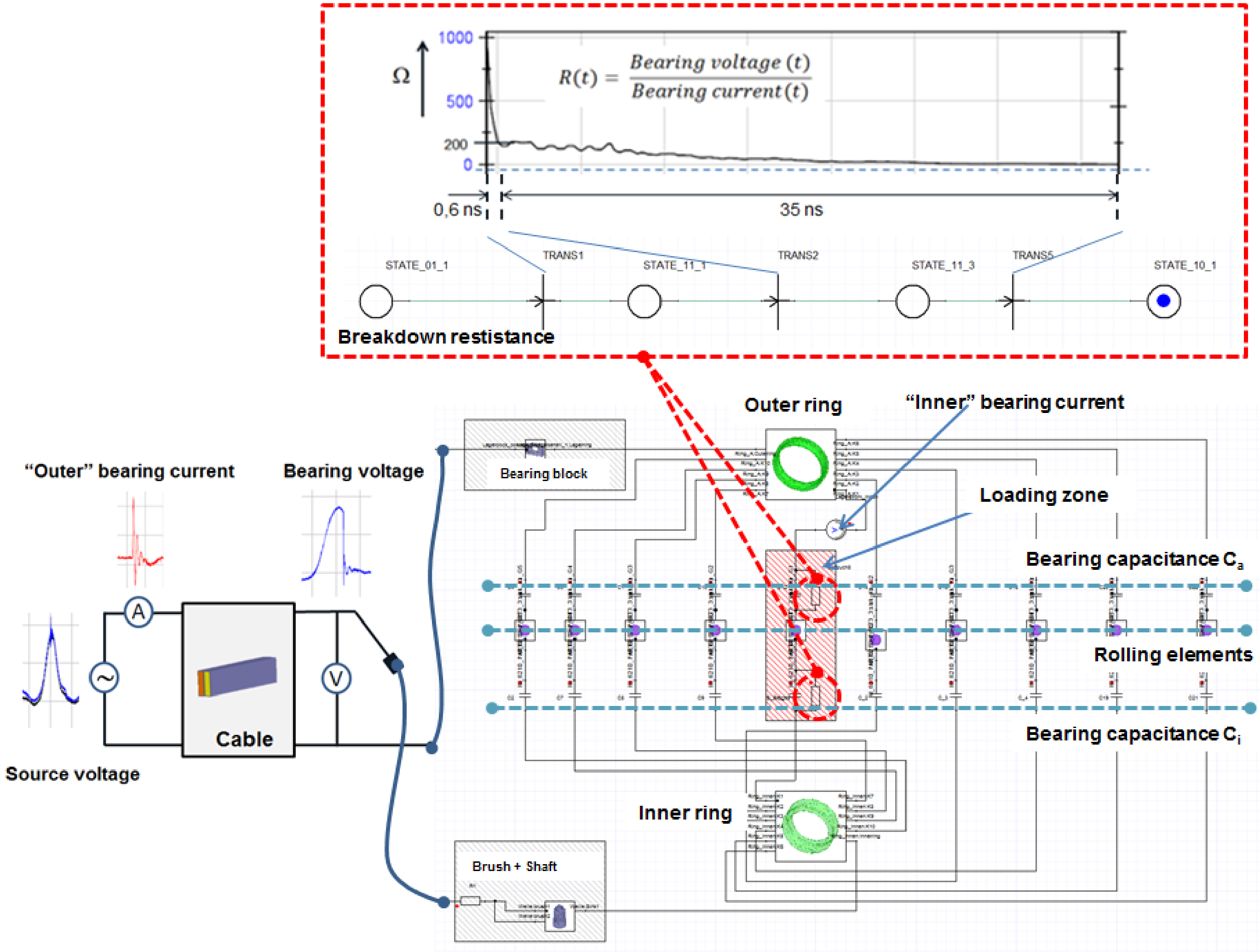

Simulation: Results (1)

SIEMENS

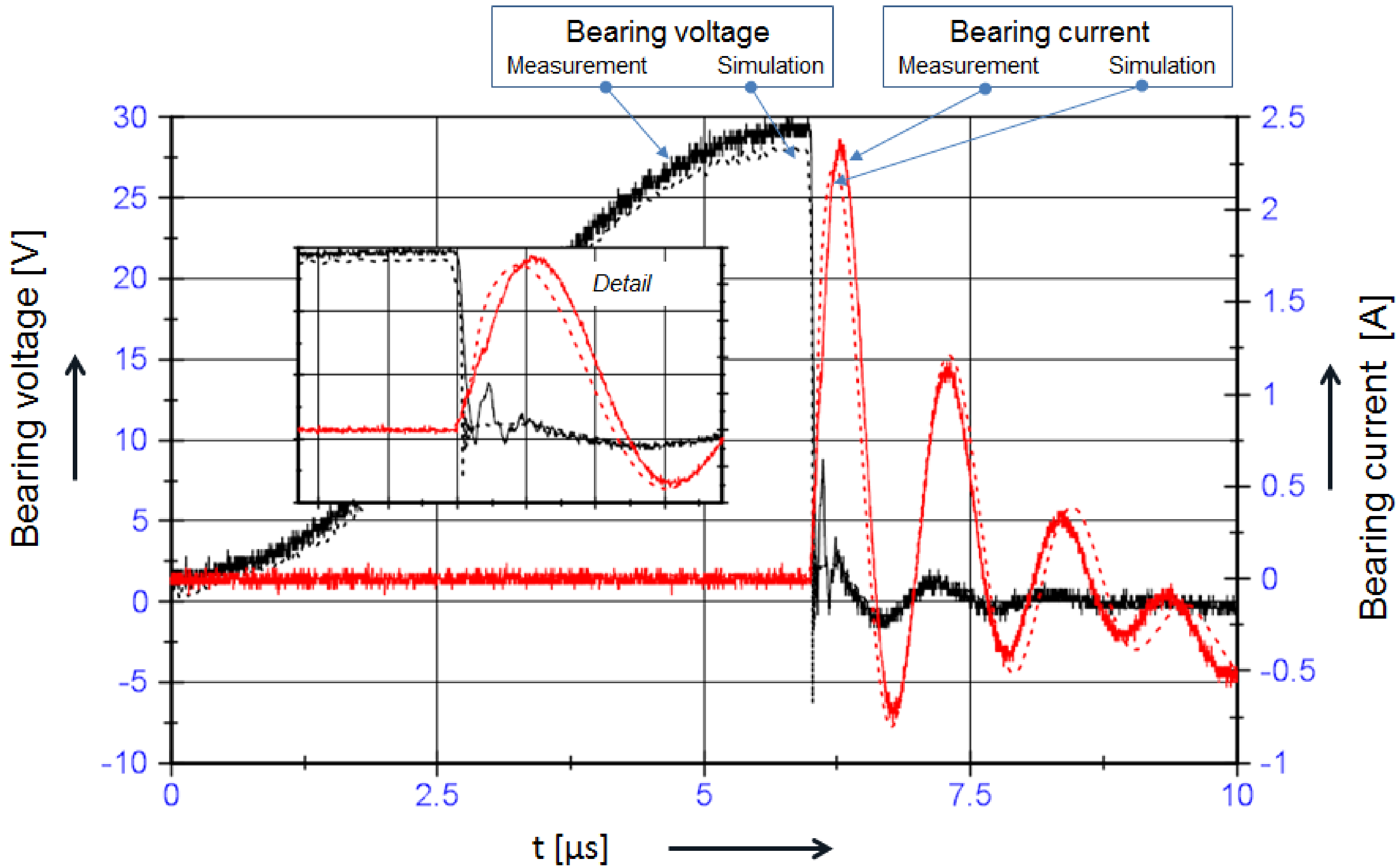

Simulation: Results (2)

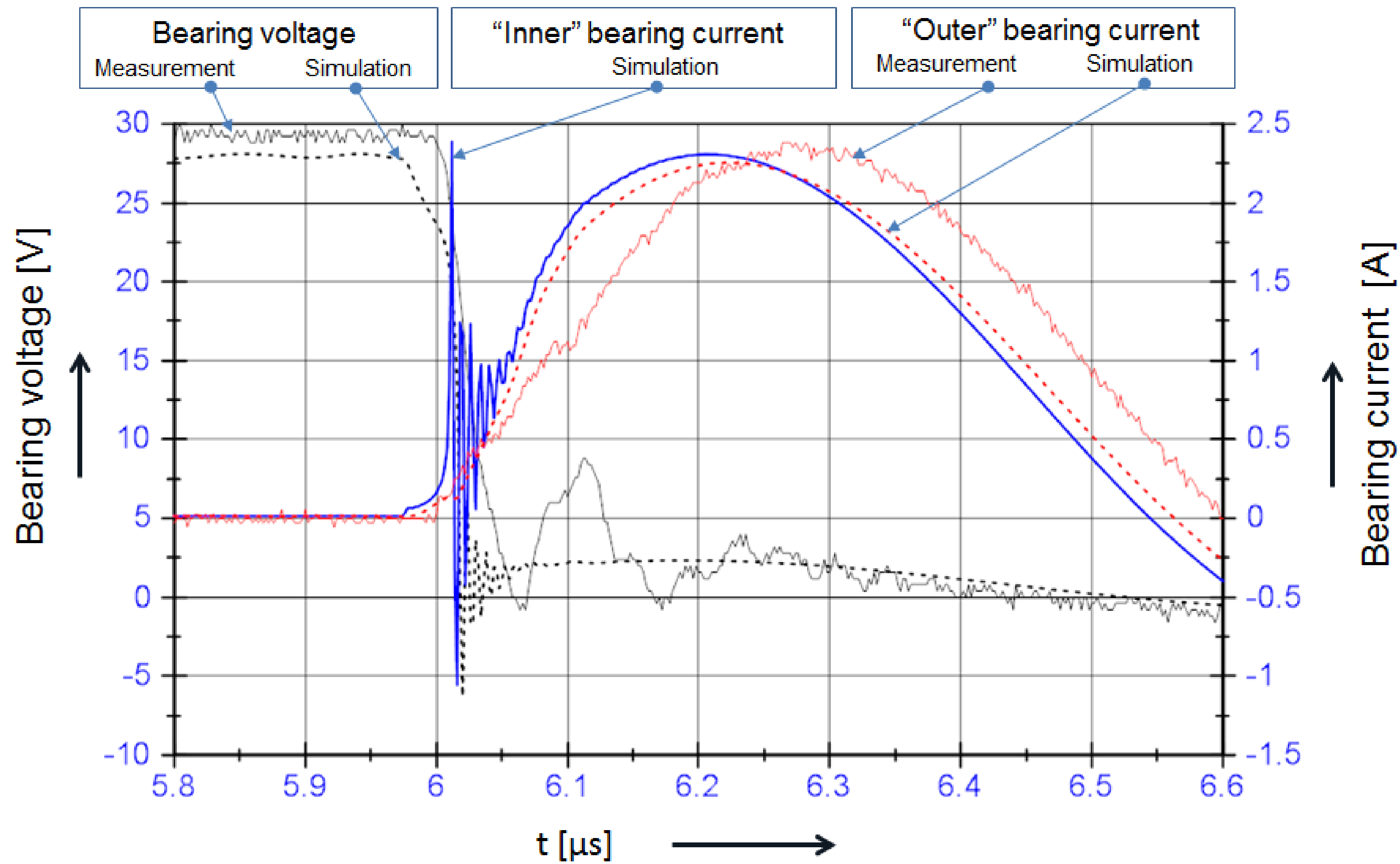

Field experience and condition monitoring: Measurement of bearing currents

SIEMENS

General measurement principle

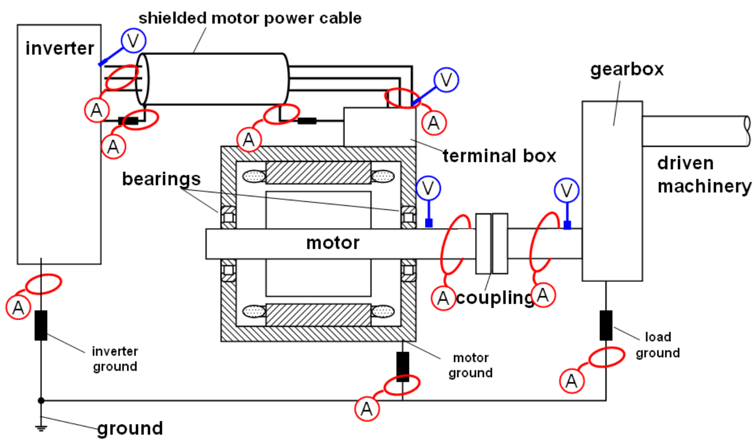

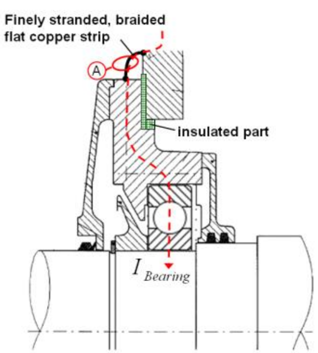

- Bearing currents cannot be measured directly
- Only at external points or indirectly
- Expensive and complex measurements

Bearing current sensor

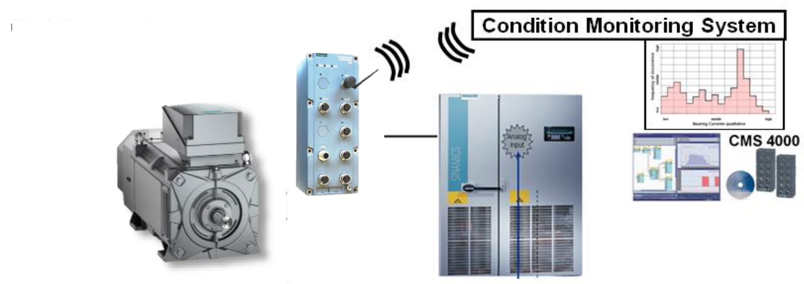

Histogram classification of the bearing current events

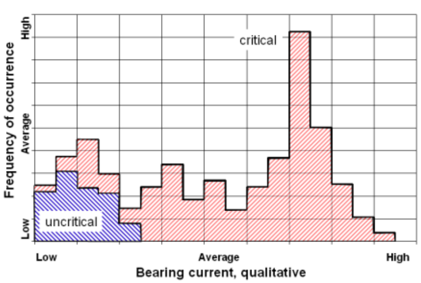

- Measuring the shaft voltage
- Calculating the bearing currents
- Evaluating the frequency of occurrence

Example for a system and field test

Integrated gear-motor configuration for cement applications

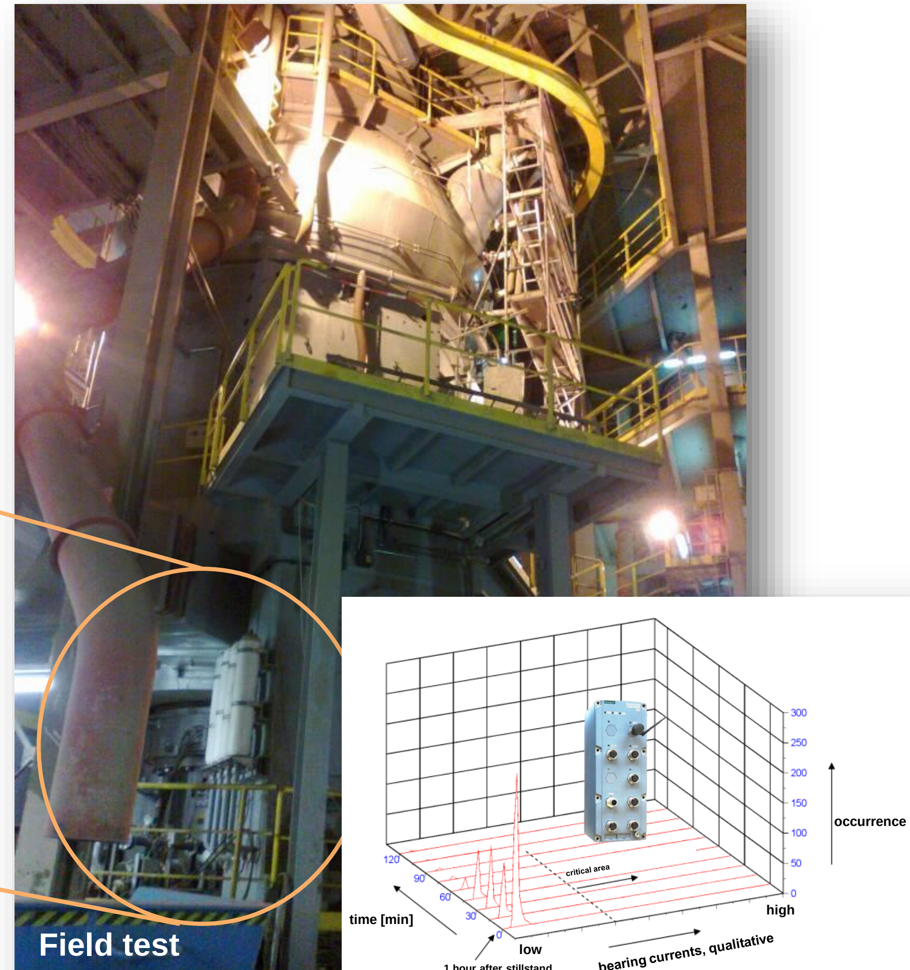

Bearing current sensor – field experience

Paper plant
Converter A
Power: 1900 kW
Motor A
SH: 560 mm

Pump
Converter B
Power: 160 kW
Motor B
SH: 315 mm

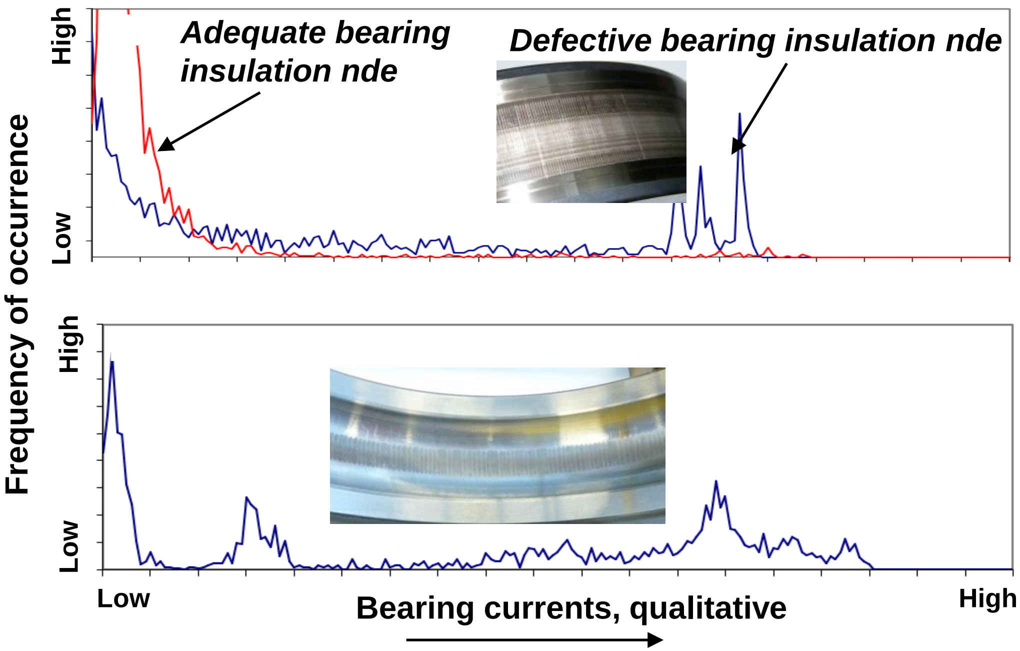

- Field tests with different system configurations
- Bearing wear due to corrugation
- The bearing current sensor provides a characteristic histogramm chart

Conclusion (2)

Bearing currents in drive systems

- Bearing currents are a system related issue.
- Current flows through the motor bearings as a result of fast-switching converters in combination with the drive system.
- Arc discharges in the lubrication gap melt or vaporize material in the raceways. Result: grey frosted raceway or corrugated patterns.
- There a different countermeasures for the three different bearing current types.

Further research activities

- Obtain field and system test data
- Identify ranges and limit values of operating parameters which favor bearing raceway damages
- Create a electrical bearing models
- Simulation of bearing currents
- Condition monitoring system for bearing currents

Content of chapter “Motor noise and vibration”

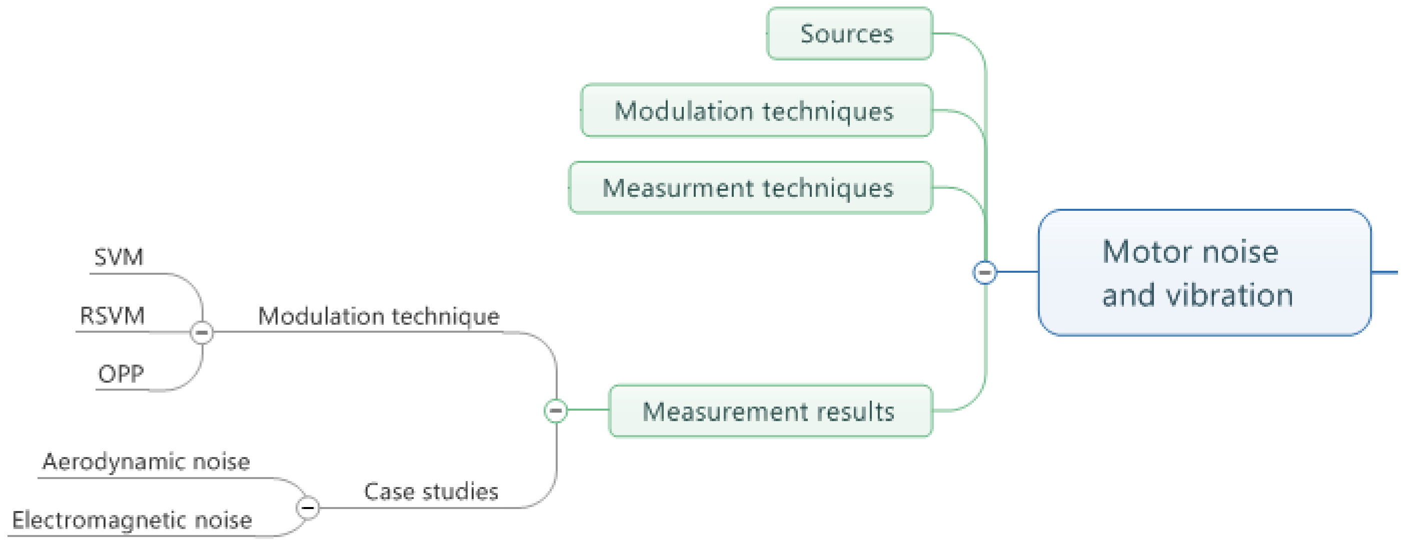

Noise sources

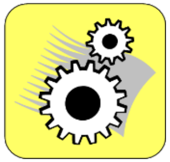

Mechanical noise

- Mainly due to bearings and their defects, shaft and rotor irregularities, e.g. rotor imbalance or shaft misalignment, as well as toothed gear trains

Aerodynamic noise

- Noise emissions due to air flow
- Cooling system of the motor (separately or self-ventilated)

Electromagnetic noise

- Noise emission caused by the electrical supply
- Radial force waves cause the laminated core to oscillate
- Magnetic force waves originating from the slot harmonics and the supply voltage harmonics

Transmission path: supply - motor

SIEMENS

Supply

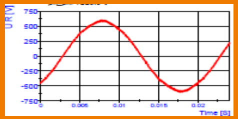

Line supply
- Sinusoidal
- Constant frequency

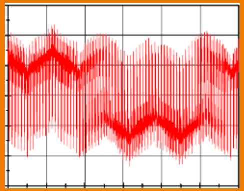

Power converter
- Pulsed voltage
- Modulation method

Motor

Winding
- Magnetic field
- Radial force wave
- Excitation of the enclosure

Stator
- Forced oscillations
- Amplified through eigenmodes
- Structure-borne noise

Enclosure surface
- Oscillating surface
- Excitation of external components
- Radiation of air borne sound

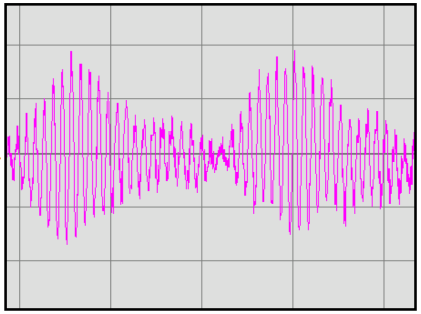

PWM converter with the space vector modulation method (SVM)

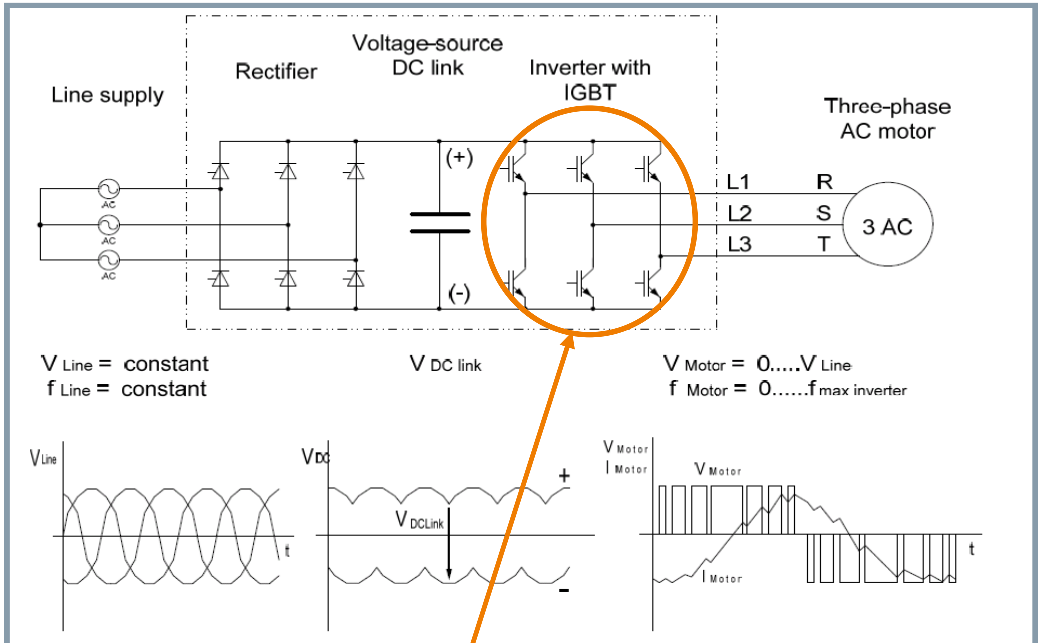

Switching states of the inverter	Phase L1	Phase L2	Phase L3
V_1	+	-	-
V_2	+	+	-
V_3	-	+	-
V_4	-	+	+
V_5	-	-	+
V_6	+	-	+
V_7	+	+	+
V_8	-	-	-

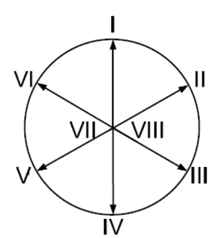

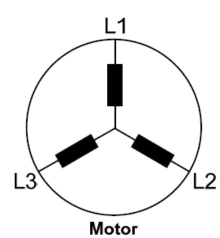

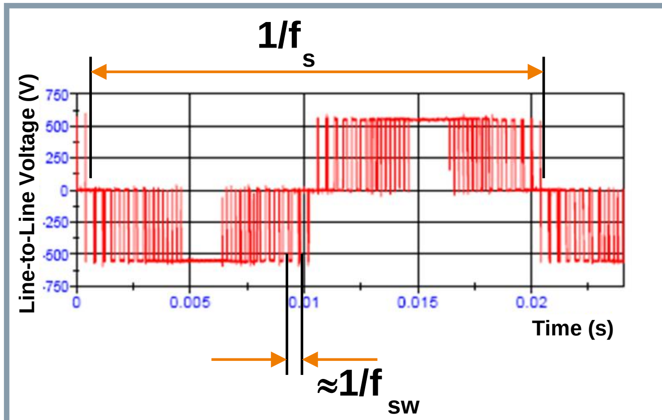

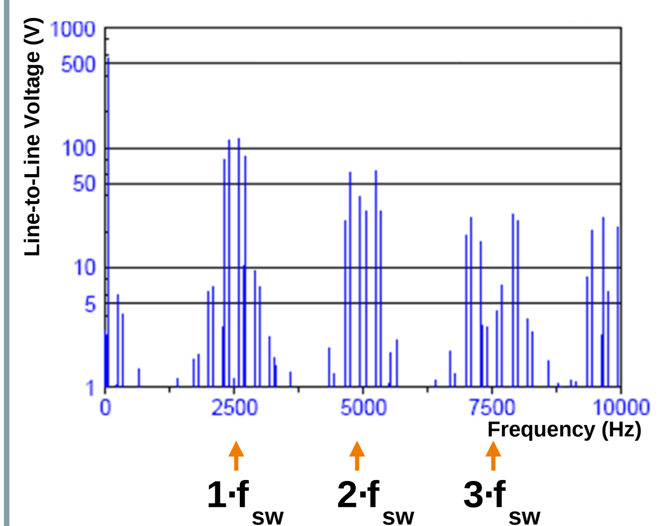

SVM – voltage and current harmonics as a function of the modulation index (theoretical computation)

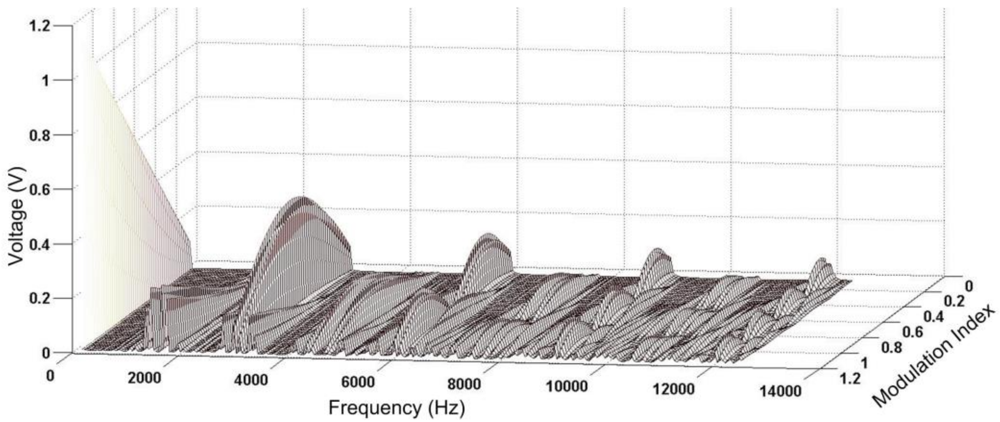

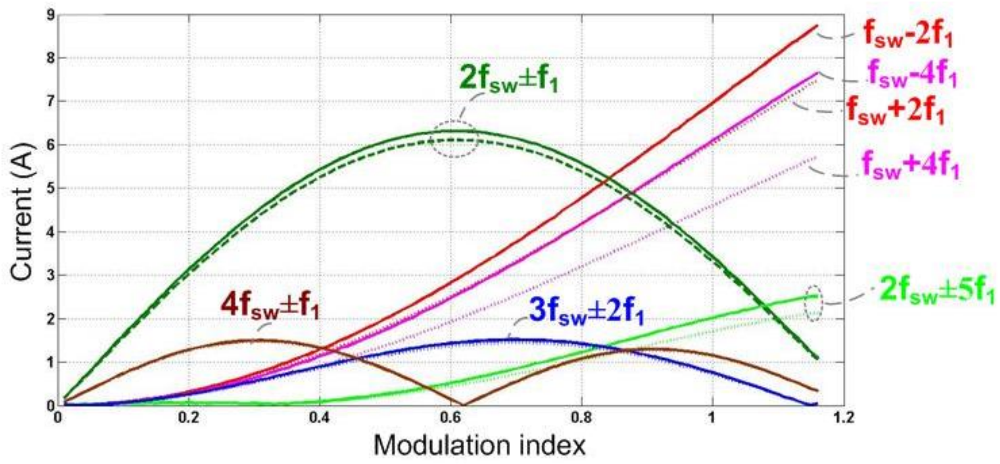

- The harmonics with frequencies $2f_{sw} \pm f_1$ dominate for modulation indexes lower than *0.8*.
- For higher modulation indexes the harmonics with frequencies $f_{sw} \pm 2f_1$ and $f_{sw} \pm 4f_1$ play a more significant role.
- Strong harmonic components concentrated in specific frequency bands around the multiples of the switching frequency.

Modulation index:

$$m = \frac{u_{UO.\nu=1}}{U_{DC}/2}$$

Randomized SVM

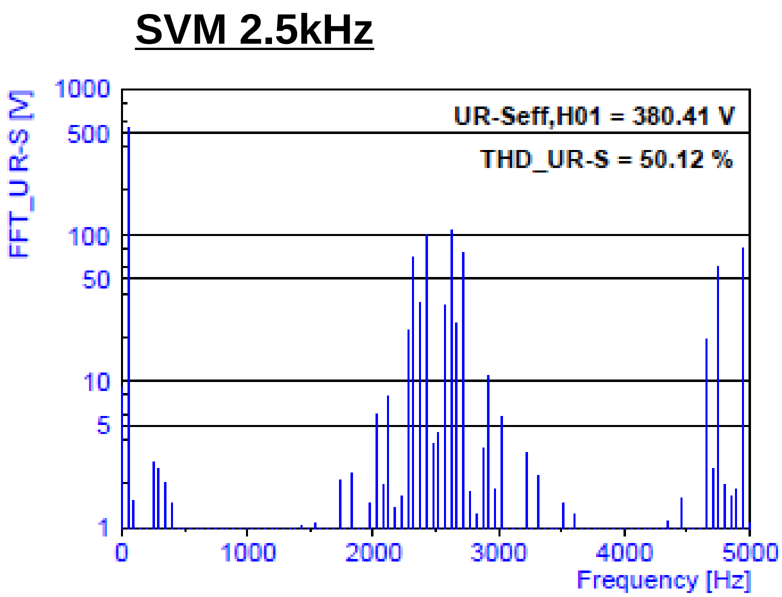

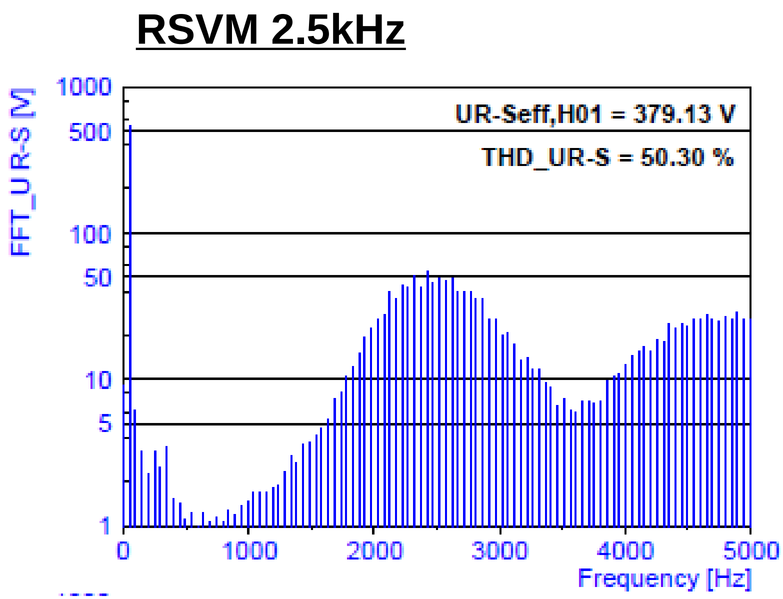

- The switching frequency is no longer constant, it randomly changes within a predefined range (e.g. 20% of the average).
- Energy spectrum spreads → less annoying sound

Inverter with optimized pulse patterns

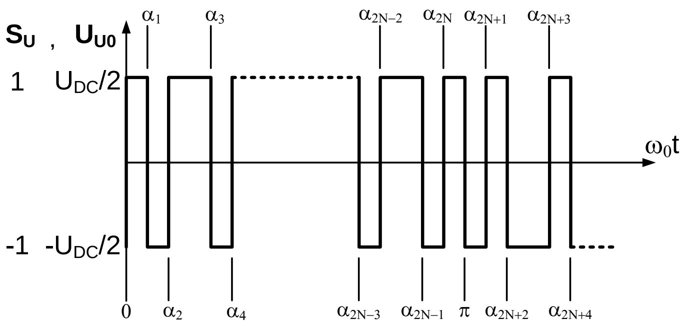

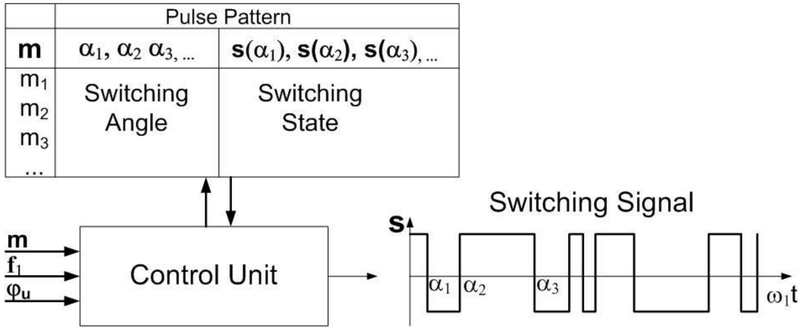

- Offline synchronous modulation technique
- The switching angles are calculated for certain optimization criteria (e.g. harmonic current)
- Stored in tables as a function of the modulation index and the inverter output frequency

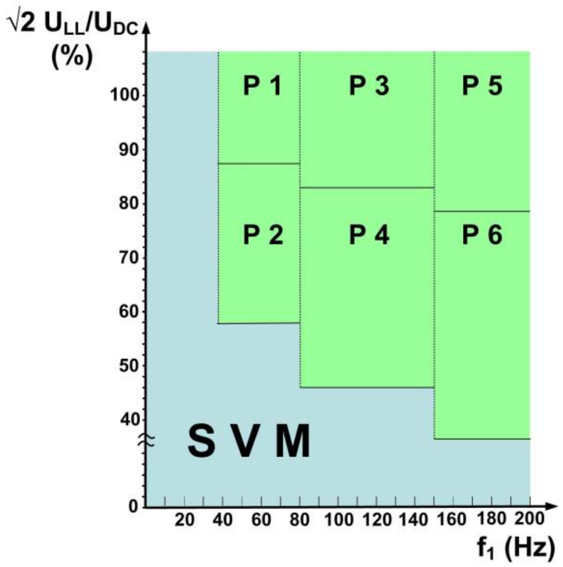

OPP – Voltage Harmonics as a Function of the Modulation Index (Theoretical Computation)

SIEMENS

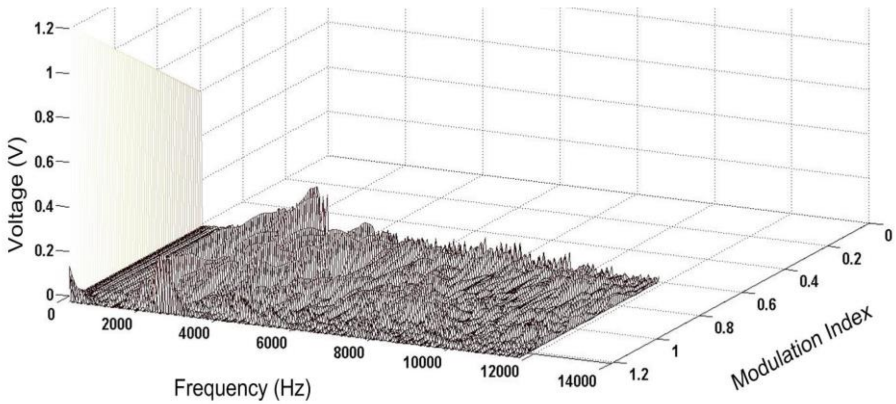

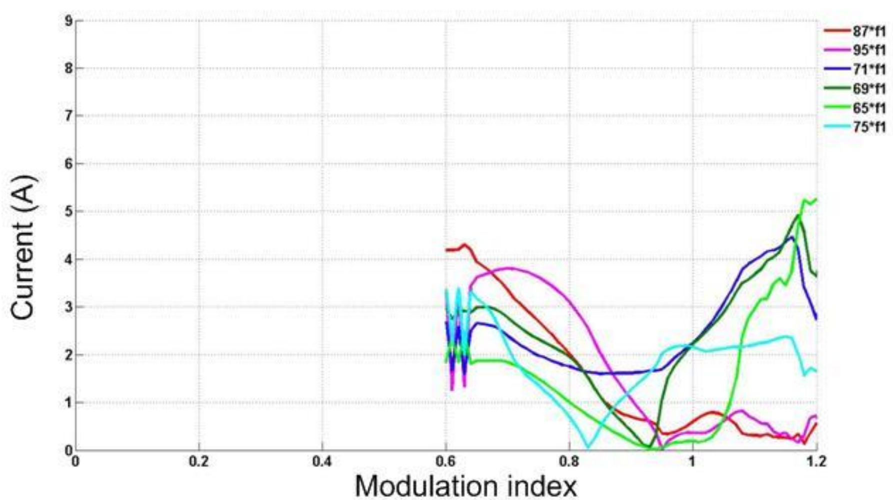

- The harmonics are distributed more uniformly in the frequency domain.
- The harmonic components are not as strong as for “online” modulation techniques
- The higher harmonics are more uniformly distributed in the frequency domain

Conclusion (1)

- Noise emitted by variable speed drives is determined not only by the motor design, but also by the motor-converter interaction.
- The inverter’s modulation significantly influences the motor’s noise emission. The modulation causes harmonic components in different frequency bands, which mainly determine the noise with electromagnetic origin emitted by the motor.
- Which one of these harmonics dominates, depends on the motor’s mechanical design (mechanical transfer function, eigenfrequencies and eigenmodes).
- Therefore the “motor-converter” system must be considered as a complete entity in order to optimize the “noise design”.

Measurement techniques

SIEMENS

Enveloping surface method

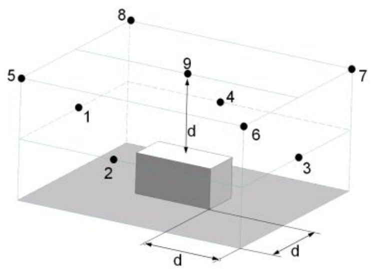

Microphone arrangement

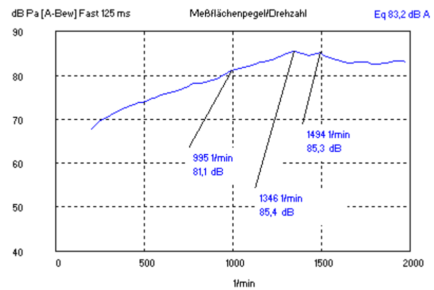

Sound pressure level vs. speed

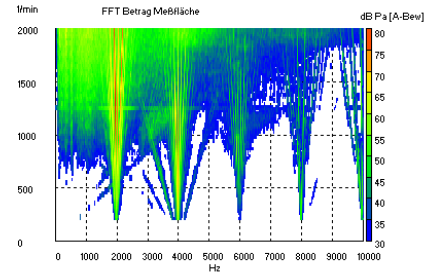

3D-Campbell diagram

Soundscaping with an acoustic camera

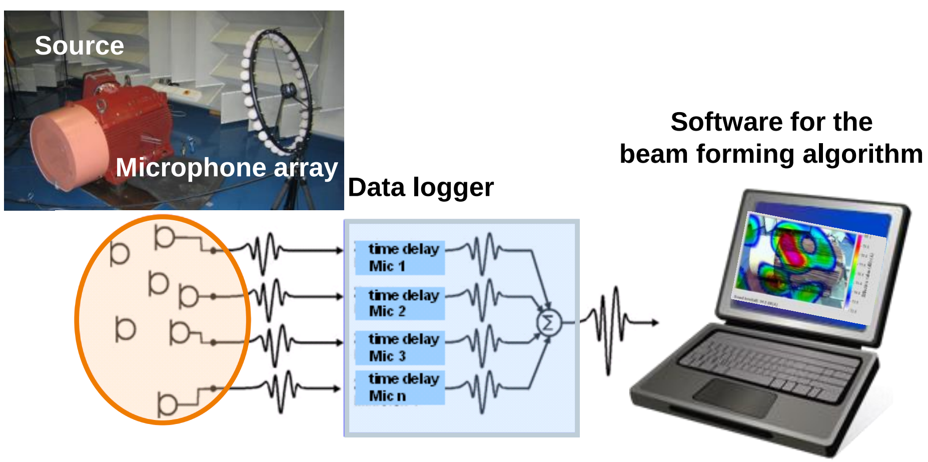

A-weighting filter

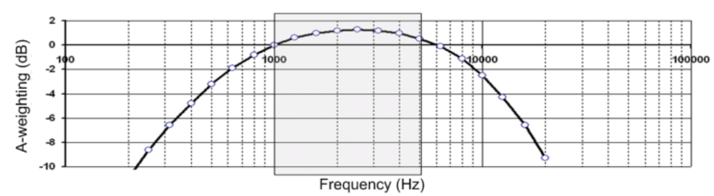

Experimental measurements
Induction motor SH 315mm

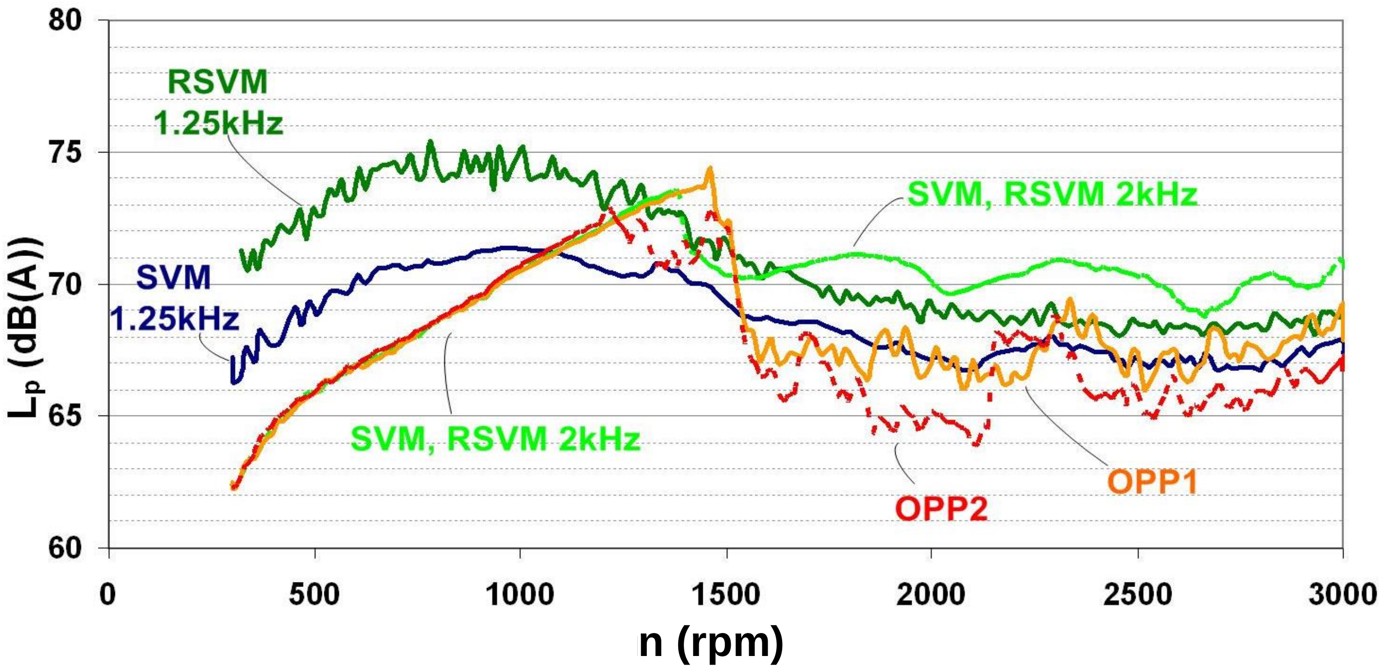

SVM:

- 1.25 kHz: noise emission determined by the harmonics at twice the switching frequency
- 2 kHz: noise emission determined by the harmonics at the switching frequency

Experimental measurements - Induction motor SH 315mm – SVM 2kHz

SIEMENS

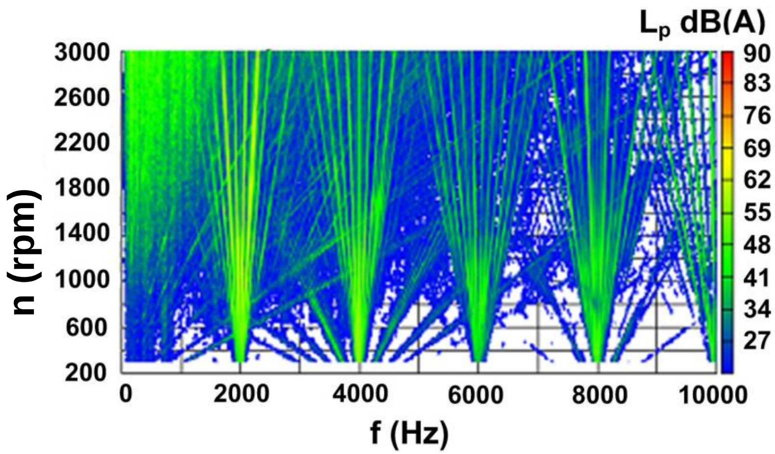

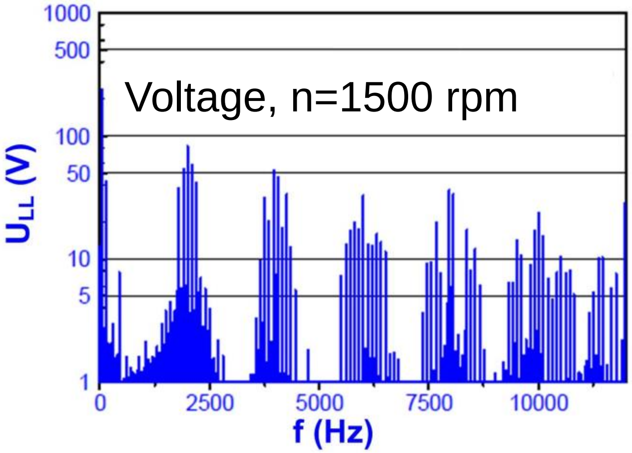

- Campbell diagram: Amplitude of harmonic components over the motor speed.
- Characteristic sideband components centered on the multiples of the switching frequency are present in the measured noise spectrum.
- Their frequency is equal to the multiples of the switching frequency plus/minus the multiples of the fundamental frequency.

Experimental measurements
Induction motor SH 315mm – RSVM 2kHz

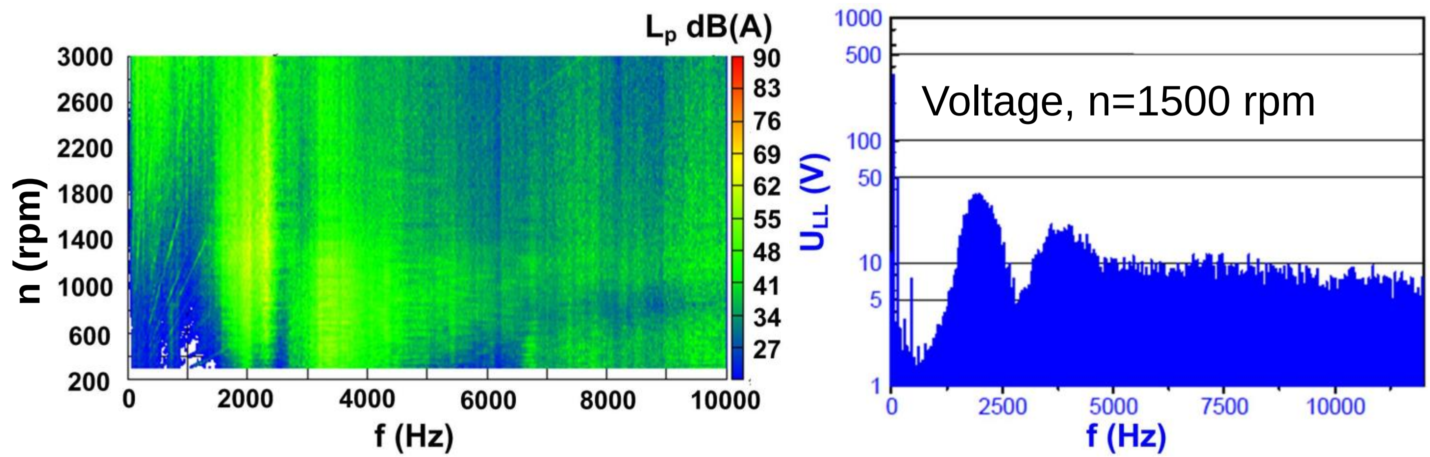

- A characteristic smearing effect is present in the spectrum of the sound pressure level of RSVM, which makes the generated noise less annoying to the human ear.
- However, the sound pressure level is not lower than that for normal SVM.

Experimental measurements
Induction motor SH 315mm – SVM 2kHz → OPP

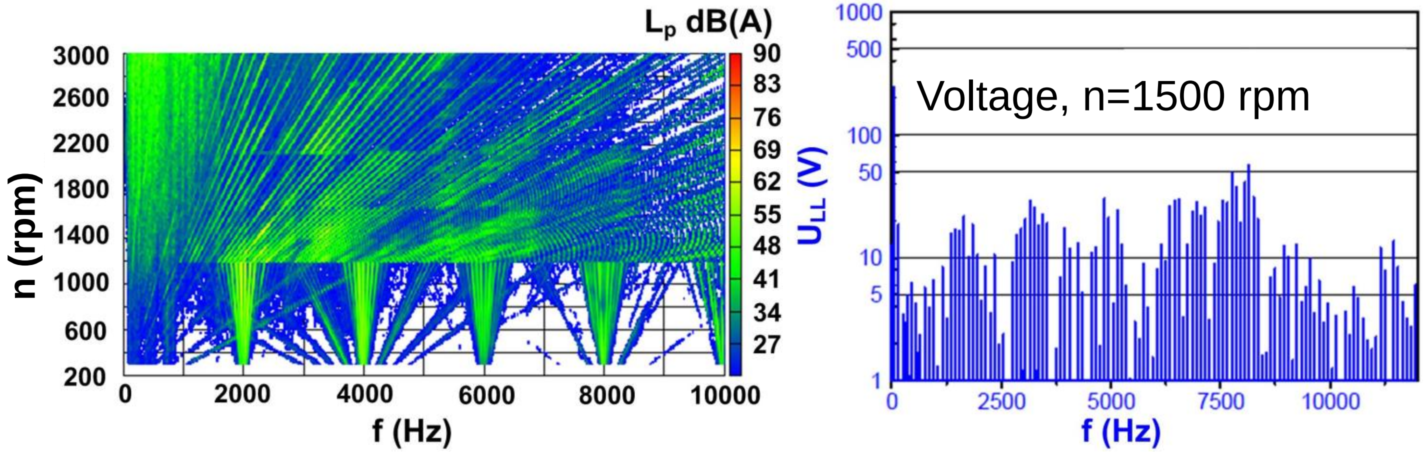

- At approx. 1200 rpm: switch from SVM to OPP
- OPP: characteristic sideband components at multiples of the fundamental frequency

Aerodynamic noise
Impact of the ventilation blades (1)

SIEMENS

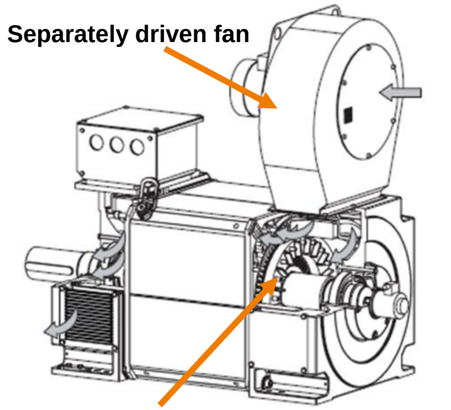

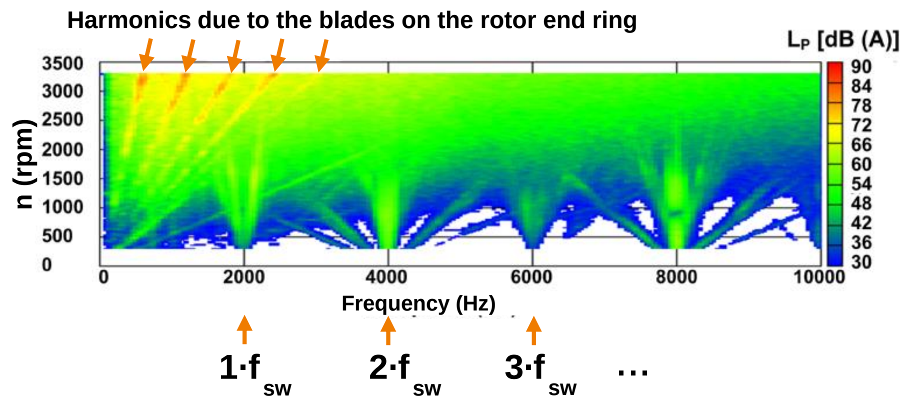

- Regions with different dominant noise sources
- Impact of the rotor blades noticeable at higher speeds
- The noise of the separately driven fan dominates at lower speeds

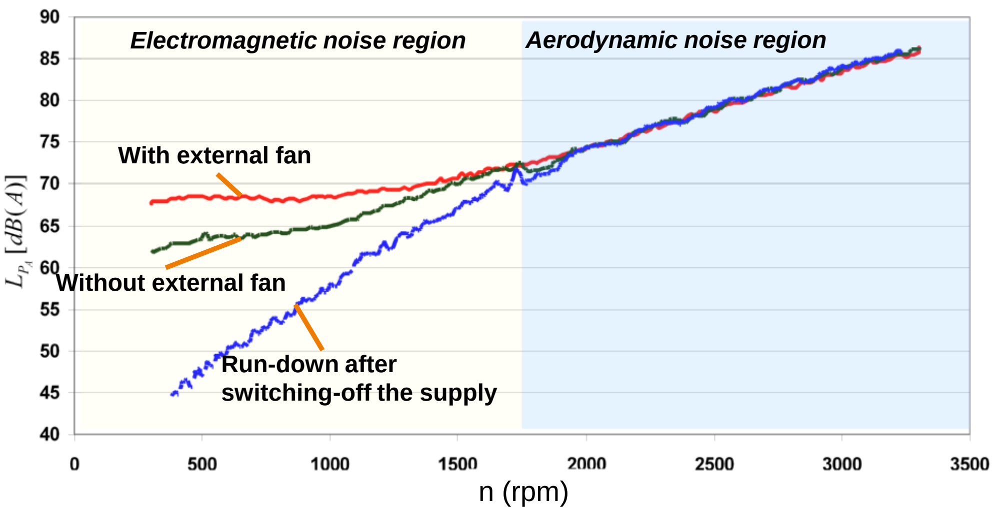

Aerodynamic noise
Impact of the ventilation blades (2)

- Filtering of the rotor blade harmonics with band–stop filters
- Estimation of the effectiveness of the modifications possible
- Subsequent measurements are in good correlation

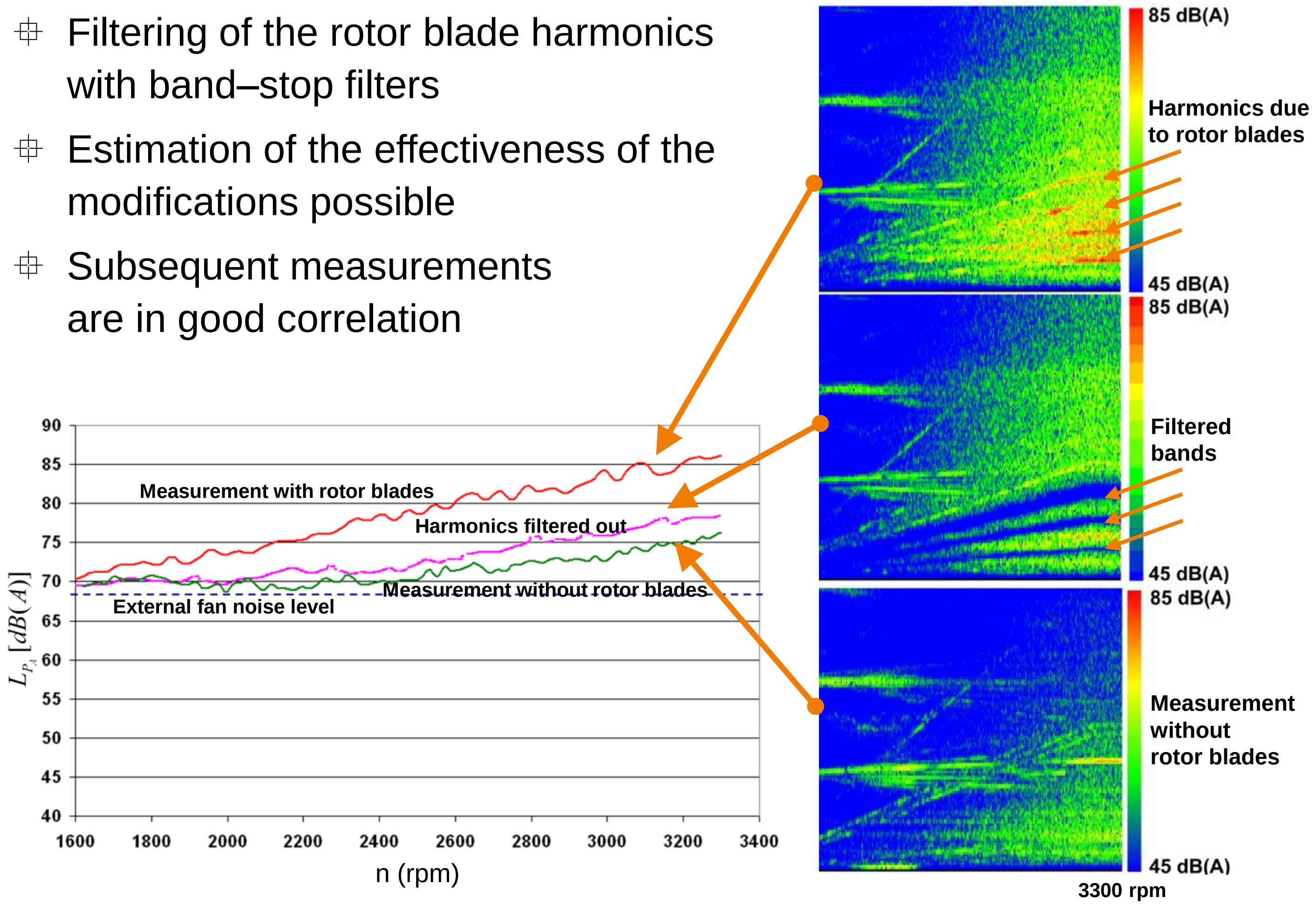

Electromagnetic noise I
Rib-cooled standard motor SH 315

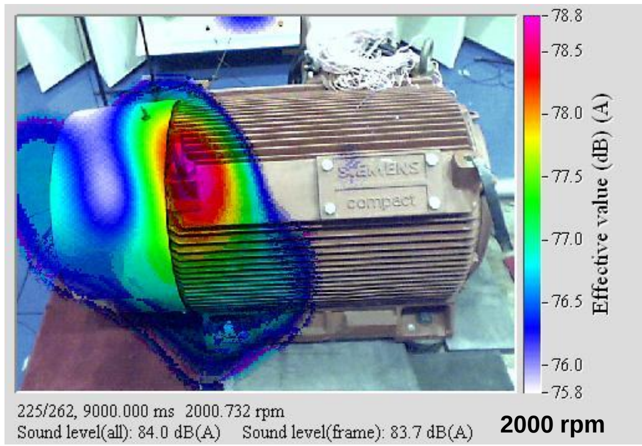

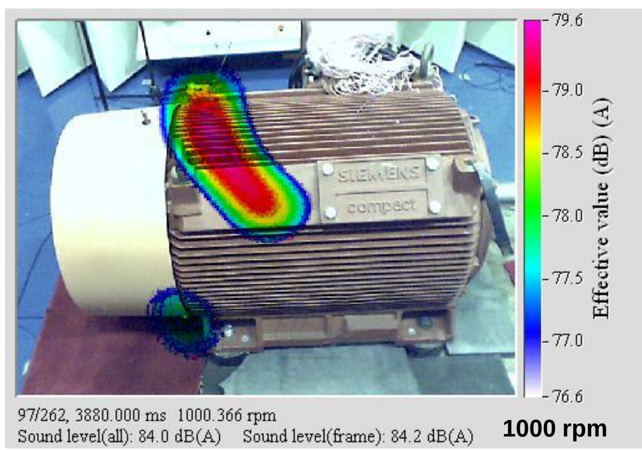

Acoustic images for f_{sw} = 2 kHz

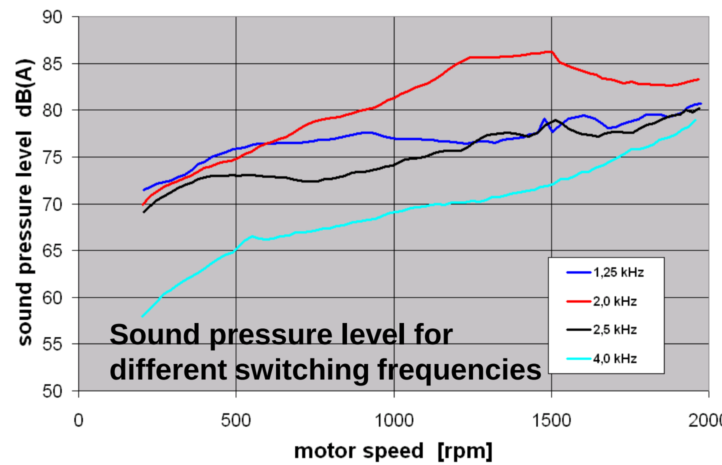

- Maximum sound pressure level for fsw = 2 kHz
- Modified parts
  - ⇨ fan cowl
  - ⇨ cooling duct

Electromagnetic noise I
Simulation of the eigenmodes

Fan cowl

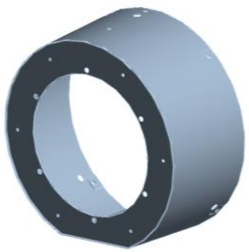

Fan cowl model

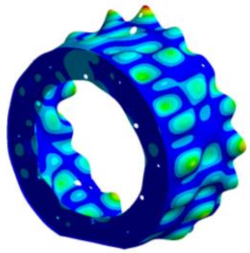

Eigenmodes around 2 kHz

- More than 200 eigenmodes between 1 and 4 kHz
- Best solution: decouple the fan cowl from the stator frame

Cooling duct

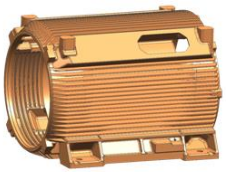

Motor frame

Cooling duct model

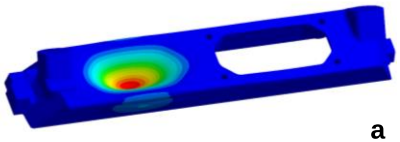

a

Calculated eigenmode at 2080Hz

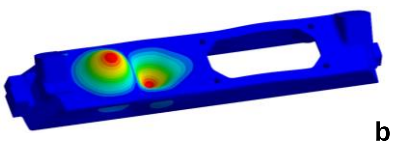

b

Calculated eigenmode at 2857Hz

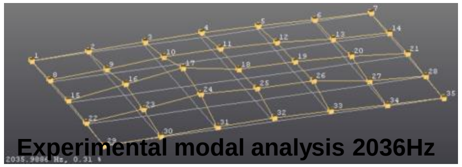

Experimental modal analysis 2036Hz

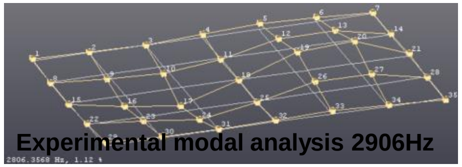

Experimental modal analysis 2906Hz

- Eigenmode “a” most critical
  Excitation through fPulse = 2 kHz
- Good correlation between simulation and experimental results
- Next step: modify cooling duct to change eigenmode “a”

Electromagnetic noise I
Modification of the cooling duct

SIEMENS

Different eigenmodes

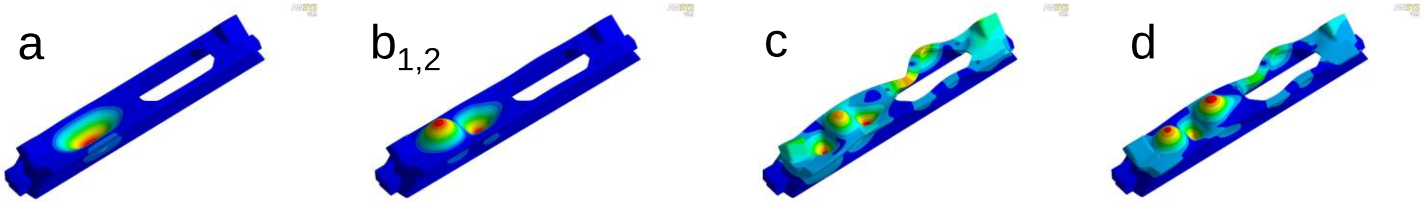

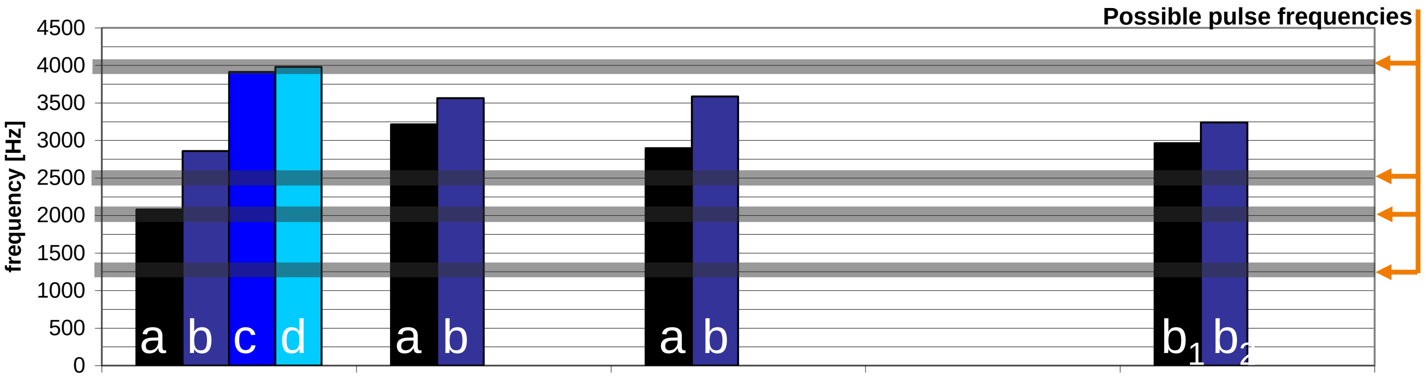

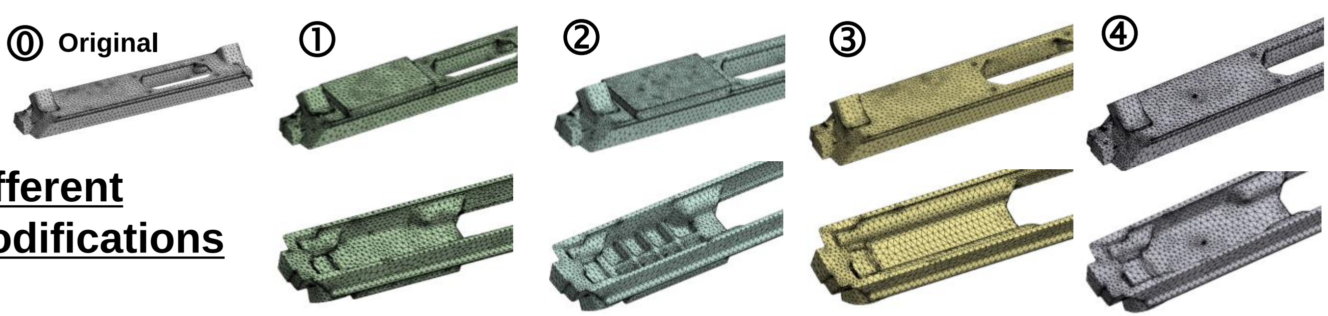

Different modifications

Electromagnetic noise I
Rib-cooled standard motor SH 315

SIEMENS

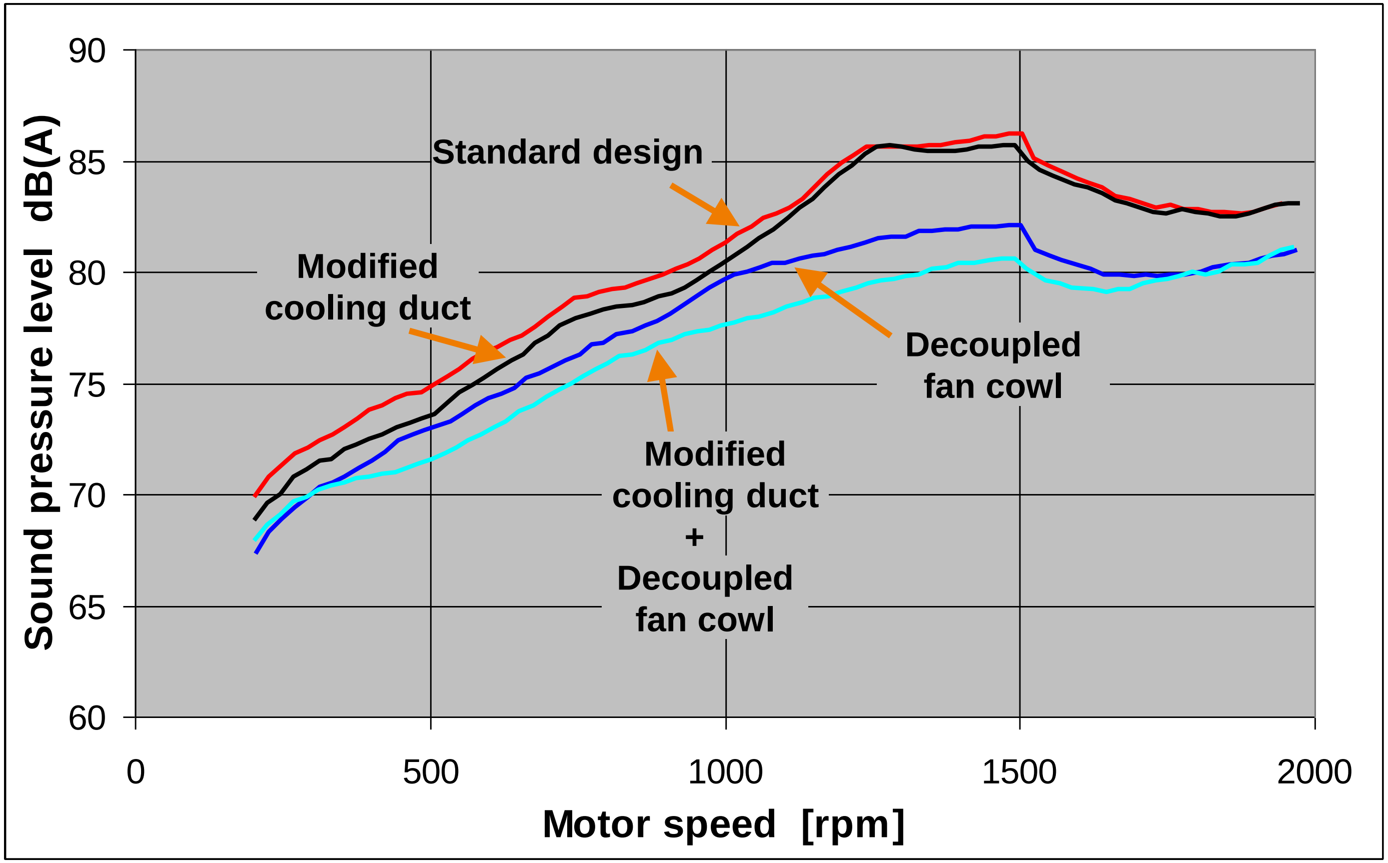

f_{sw} = 2 kHz

Electromagnetic noise I
Rib-cooled standard motor SH 315

SIEMENS

Standard design | Modified cooling duct

Standard design

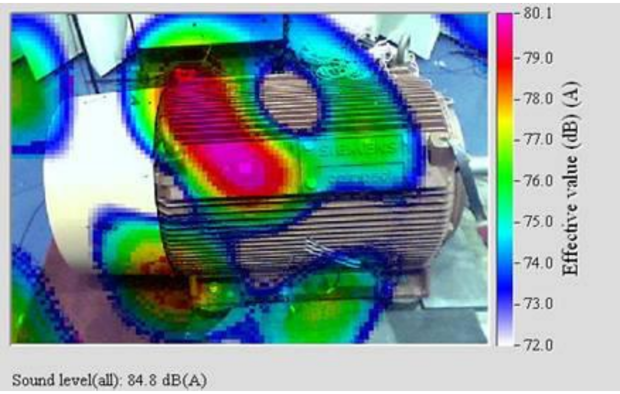

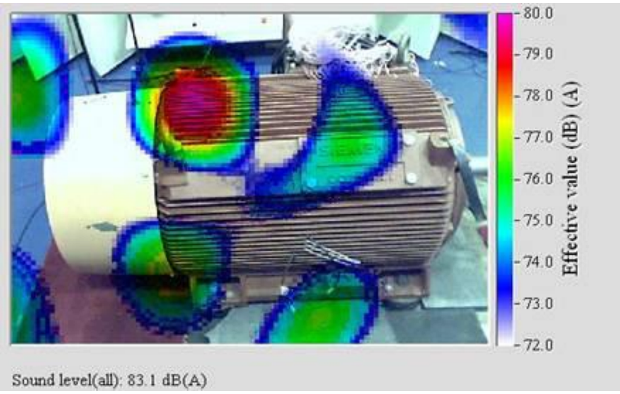

Decoupled fan cowl

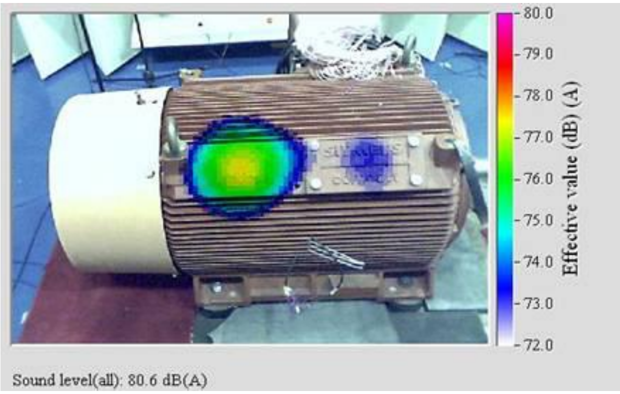

f_{sw} = 2 kHz

Speed 1000 1/min

Electromagnetic noise II
Temperature dependency

SIEMENS

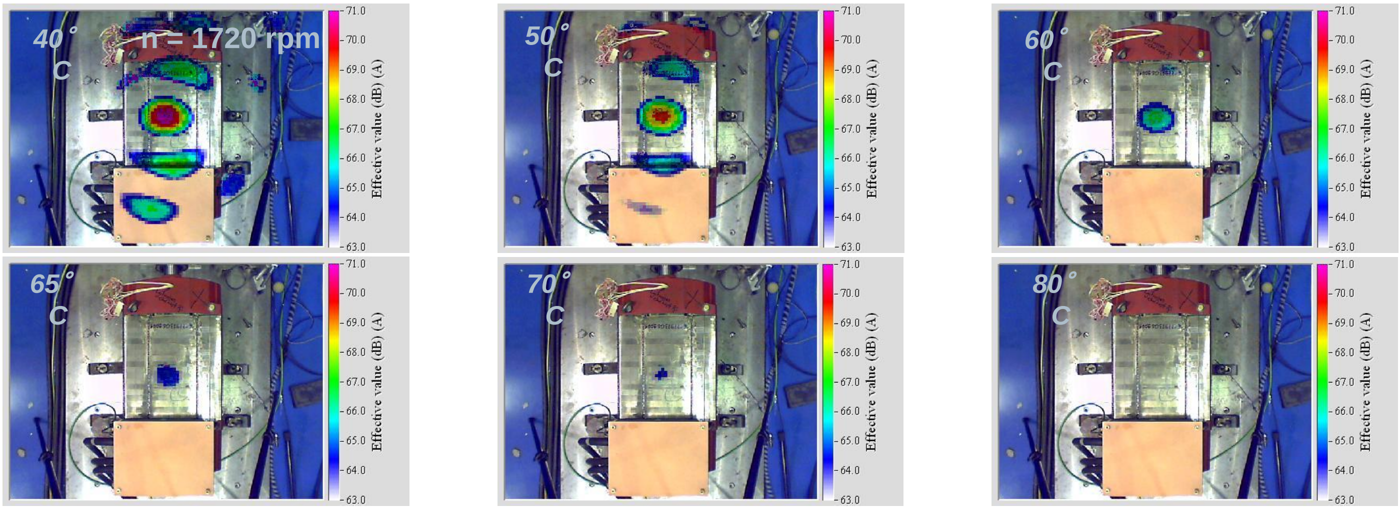

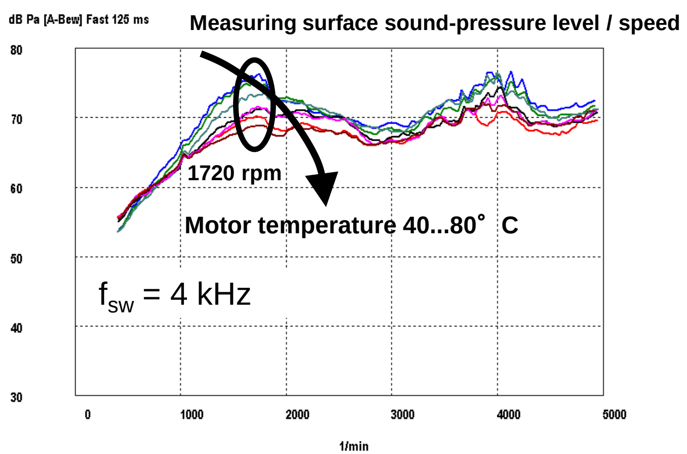

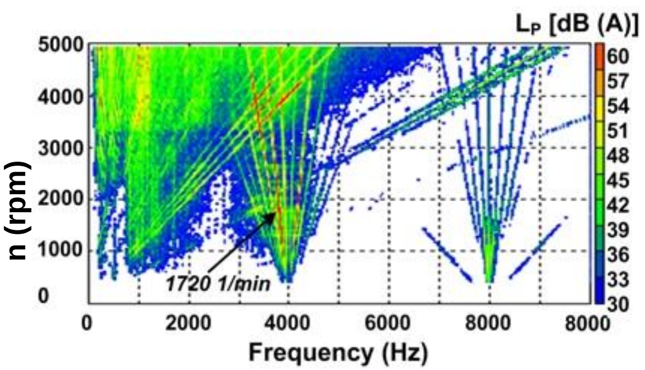

Temperature-dependent change of resonance points and damping

Electromagnetic noise II
Temperature dependency

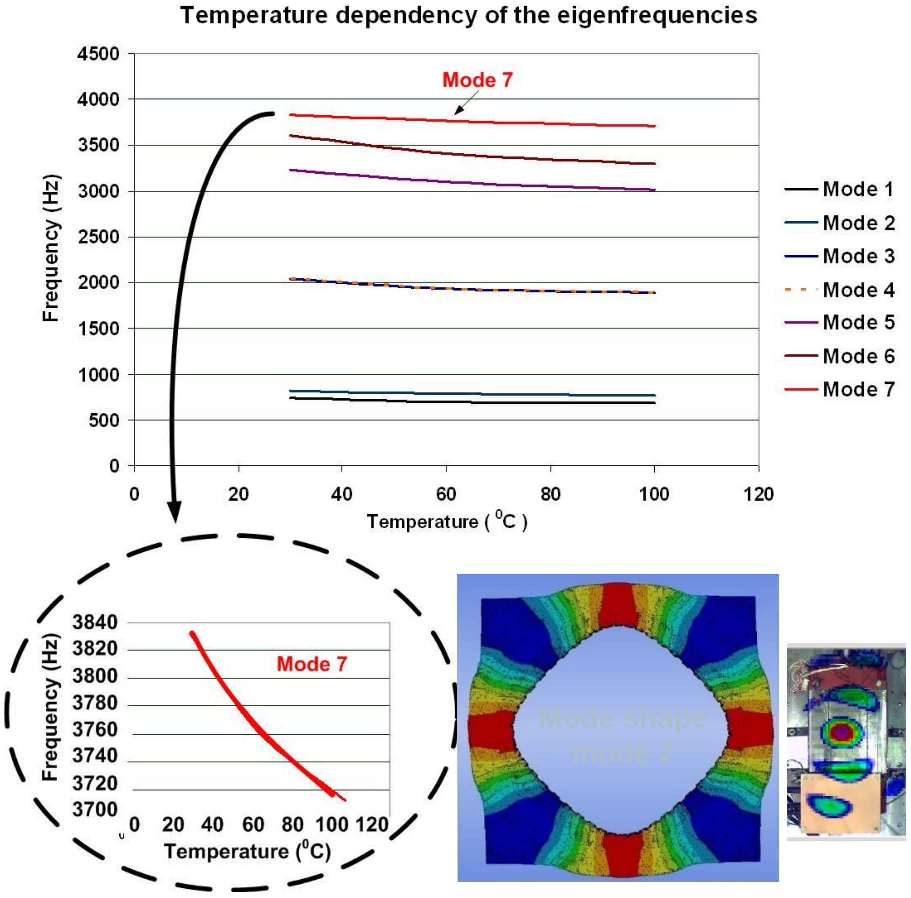

- Simulation of the mode shapes taking into account the winding, the casting resin and the stator iron
- Mode 7 dominates in the frequency region being considered
- The change of the E-module of the casting resin affects the eigen-frequencies and the damping
- This results in strongly temperature-dependent noise radiation in the speed range being considered

Conclusion (2)

Consideration of the complete drive system

- Power converter / motor
- Determination of possible noise sources

Combination of measurement techniques

- Envelope surface method and sound-mapping

Analysis of the affected motor parts

- Analysis of the excitation sources
- Focus on the region of the maximum noise radiation

Determination of suitable solutions

- Simulation of the system behavior in the regions of interest
- “Alignment” of measurement and theoretical calculations
- Determination of possible corrective measures and validation through simulation

Comparison measurement – simulation – calculations

- For validation of the improvements
- For adjustments of the simulation tool

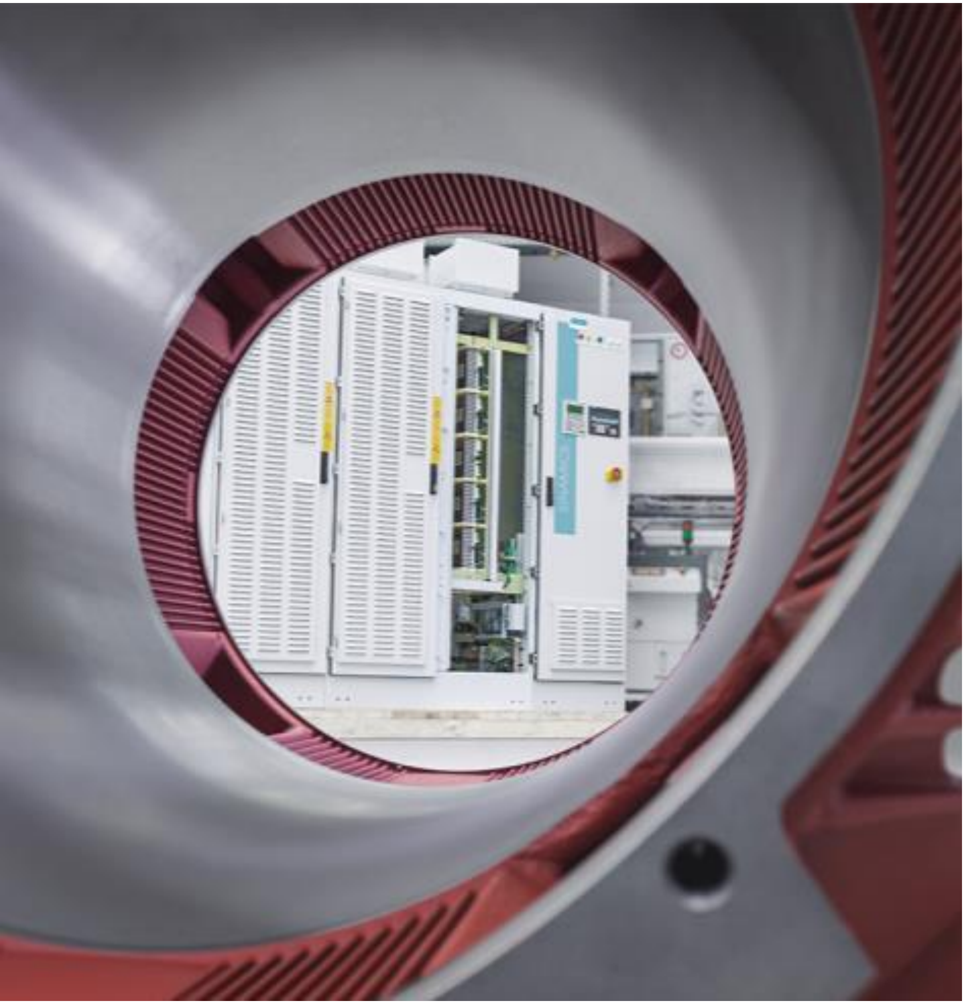

Hans Tischmacher
Senior Key Expert
PD LD P R&D 31

Vogelweiherstr. 1-15
90441 Nuremberg

E-mail:
hans.tischmacher@siemens.com

siemens.de/large-drives